A new species of *Metopocetus* (Cetacea, Mysticeti, Cetotheriidae) from the Late Miocene of the Netherlands

Felix Georg Marx, Mark E. J. Bosselaers, Stephen Louwye

The family Cetotheriidae has played a major role in recent discussions of baleen whale phylogenetics. Within this group, the enigmatic, monotypic *Metopocetus durinasus* has been interpreted as transitional between herpetocetines and other members of the family, but so far has been restricted to a single, fragmentary cranium of uncertain provenance and age. Here, we expand the genus and shed new light on its phylogenetic affinities and functional morphology by describing *Metopocetus hunteri* sp. nov. from the Late Miocene of the Netherlands. Unlike the holotype of *M. durinasus*, the material described here is confidently dated and preserves both the tympanic bulla and additional details of the basicranium. *M. hunteri* closely resembles *M. durinasus*, differing primarily in its somewhat less distally expanded compound posterior process of the tympanoperiotic. Both species are characterised by the development of an unusually large fossa on the ventral surface of the paroccipital process, which extends anteriorly on to the compound posterior process and completely floors the facial sulcus. In life, this enlarged fossa may have housed the posterior sinus and/or the articulation of the stylohyal. Like other cetotheriids, *Metopocetus* also bears a well-developed, posteriorly-pointing dorsal infraorbital foramen near the base of the ascending process of the maxilla, the precise function of which remains unclear.

A new species of *Metopocetus* (Cetacea, Mysticeti, Cetotheriidae) from the Late Miocene of the Netherlands

Felix G. Marx[1] Mark Bosselaers[2,3] and Stephen Louwye[4]

[1]Department of Geology and Palaeontology, National Museum of Nature and Science, 4-1-1 Amakubo, Tsukuba 305-0005, Japan. Corresponding author: felix.marx@otago.ac.nz.

[2]Directorate of Earth and History of Life, Royal Belgian Institute of Natural Sciences, Rue Vautier 29, 1000 Brussels, Belgium, mark.bosselaers@telenet.be.

[3]Zeeland Royal Society of Sciences, 4331 JE Middelburg, the Netherlands.

[4]Research Unit Palaeontology, Ghent University, Krijgslaan 281/S8, 9000 Ghent, Belgium, stephen.louwye@ugent.be.

Note to reviewers: illustrated cladistic scorings for the new material are available from MorphoBank, project 2225. They can be accessed for review purposes by visiting www.morphobank.org and entering the following on the login page:

e-mail address: 2225
password: Metopocetusreview

The data will be made publicly available as soon as soon as the paper is published.

Abstract: The family Cetotheriidae has played a major role in recent discussions of baleen whale phylogenetics. Within this group, the enigmatic, monotypic *Metopocetus durinasus* has been interpreted as transitional between herpetocetines and other members of the family, but so far has been restricted to a single, fragmentary cranium of uncertain provenance and age. Here, we expand the genus and shed new light on its phylogenetic affinities and functional morphology by describing *Metopocetus hunteri* sp. nov. from the Late Miocene of the Netherlands. Unlike the holotype of *M. durinasus*, the material described here is confidently dated and preserves both the tympanic bulla and additional details of the basicranium. *M. hunteri* closely resembles *M. durinasus*, differing primarily in its somewhat less distally expanded compound posterior process of the tympanoperiotic. Both species are characterised by the development of an unusually large

fossa on the ventral surface of the paroccipital process, which extends anteriorly on to the compound posterior process and completely floors the facial sulcus. In life, this enlarged fossa may have housed the posterior sinus and/or the articulation of the stylohyal. Like other cetotheriids, *Metopocetus* also bears a well-developed, posteriorly-pointing dorsal infraorbital foramen near the base of the ascending process of the maxilla, the precise function of which remains unclear.

INTRODUCTION

The Cetotheriidae play a crucial role in the evolution of baleen whales (Mysticeti). Long degraded to the state of a wastebasket taxon comprising nearly all fossil toothless mysticetes, the past decade saw the family restored to its original definition – *Cetotherium* Brandt, 1843 and relatives – within a phylogenetic context (Bouetel & de Muizon 2006; Brandt 1873; Steeman 2007; Whitmore & Barnes 2008). The importance of this prominent family lies not only in its rather disparate morphology, which is clearly distinct from that of all living species and persisted as late as the Pleistocene (Boessenecker 2013), but also the still controversial idea that it may have given rise to the most enigmatic of the extant mysticetes, the pygmy right whale *Caperea marginata* Gray, 1846 (Fordyce & Marx 2013; Marx et al. 2013; Marx & Fordyce 2015). The phylogenetic position of the family relative to crown mysticetes remains a matter of debate, as does its exact composition and the interrelationships of the included species (Bisconti 2015; Bouetel & de Muizon 2006; Deméré et al. 2008; El Adli et al. 2014; Gol'din & Startsev 2014; Gol'din et al. 2014; Kimura & Hasegawa 2010; Marx & Fordyce 2015; Steeman 2007).

There is wide agreement on the existence of at least one subfamily, Herpetocetinae, within Cetotheriidae, comprising at least the closely related genera *Herpetocetus* Van Beneden, 1872 and *Nannocetus* Kellogg, 1929 (Whitmore & Barnes 2008). The remaining cetotheriids are often partially or entirely lumped into the subfamily Cetotheriinae, although the definition of this grouping tends to vary across analysis (Bisconti 2015; El Adli et al. 2014; Gol'din & Startsev 2014; Marx & Fordyce 2015; Tarasenko & Lopatin 2012). Within this context, the genus *Metopocetus* Cope, 1896 has been interpreted as a potentially intermediate form linking herpetocetines and cetotheriines (Whitmore & Barnes 2008); however, so far this taxon has had

an unstable phylogenetic history (El Adli et al. 2014; Gol'din & Startsev 2014; Marx & Fordyce 2015; Steeman 2007).

At least in part, the uncertainty surrounding *Metopocetus* likely reflects the incomplete nature of the available material: to date, the genus has remained restricted to its type species, *M. durinasus* Cope, 1896, which in turn is based on just a single, fragmentary cranium (USNM 8518) missing the rostrum, tympanic bulla and much of the basicranium (Cope 1896; Kellogg 1968; Whitmore & Barnes 2008). The affinities of the only other putative occurrence of *Metopocetus*, "*M.*" *vandelli* (Van Beneden, 1871) from the Late Miocene of Portugal (Kellogg 1941), are doubtful (El Adli et al. 2014; Gol'din & Startsev 2014; Whitmore & Barnes 2008). Compounding these issues further are the lack of clear stratigraphic and provenance data for USNM 8518, which may have been derived from either Langhian or Tortonian deposits (Case 1904; Kellogg 1931; Kellogg 1968).

Here, we describe a new species of *Metopocetus* from the Late Miocene of north-western Europe (the Netherlands), the first material clearly representing this genus besides *M. durinasus*, and its first occurrence outside North America (Fig. 1). Unlike USNM 8518, the specimen described here is confidently dated and preserves both the tympanic bulla and additional details of the basicranium, thus providing new insights into cetothere phylogeny and functional morphology.

MATERIAL AND METHODS

Collection, preparation and phylogenetic analysis

The specimen was collected in 1987 by O. Stolzenbach and mechanically prepared by K. Post and one of the authors (MB). Morphological terminology follows Mead & Fordyce (2009), unless indicated. For the figures, photographs of the specimen were digitally stacked in Photoshop CS6. To determine the phylogenetic position of our new material, we added the specimen to the recently published matrix of Marx & Fordyce (2015: fig. 2). Further, we also included "*Metopocetus*" *vandelli* (holotype MUHNAC A1) and the morphologically similar "*Aulocetus*" *latus* Kellogg, 1941 (holotype MUHNAC A2) to determine their placement relative

to *Metopocetus* proper. Both of these taxa are known only from Adiça (Lower Tagus Basin, Portugal) and were recovered from Late Miocene strata correlative with Cotter's lithostratigraphic zone VIIb, dated to ca 9.5–8.5 Ma (Antunes et al. 2000; Estevens & Antunes 2004; Kellogg 1941; Pais et al. 2008).

Besides these additions, we retained all of the previous taxa and codings, with two exceptions: in the previous analysis "*Cetotherium*" *megalophysum* Cope, 1895, was coded as having the posterior end of the ascending processes of the maxillae contact each other in dorsal view (char 69:2), and consequently as "NA" for character 68, "Triangular wedge of frontal separating ascending process of maxilla from nasal or premaxilla". Further observations have revealed these observations to be inaccurate, and we here correct them to states 68:0 (triangular wedge of frontal absent) and 69:1 (ascending processes of maxillae converging towards the midline and separated by nasals only). The analysis was run in MrBayes 3.2.6, on the Cyberinfrastructure for Phylogenetic Research (CIPRES) Science Gateway (Miller et al. 2010). Our new morphological codings and the full matrix are available from MorphoBank, project 2225 (full matrix stored in the "Documents" section) and as part of the online supplementary material.

Age determination

To determine the age of the new specimen, we searched a sample of in situ sediment recovered from the cranium for biostratigraphically informative palynomorphs. The extraction procedure followed the standard protocol of Louwye et al. (2007), and involved successive treatments with HCl and HF to remove carbonates and silicates, respectively. No oxidation or ultrasonic treatment was applied to avoid damage and selective loss of species. The organic residue was mounted with glycerine jelly on two microscope slides, which were then systematically scanned for palynomorphs. Nomenclature of the dinoflagellate cysts follows Fensome et al. (2008).

Nomenclatural acts

The electronic version of this article in Portable Document Format (PDF) will represent a published work according to the International Commission on Zoological Nomenclature (ICZN), and hence the new names contained in the electronic version are effectively published under that Code from the electronic edition alone. This published work and the nomenclatural acts it

contains have been registered in ZooBank, the online registration system for the ICZN. The ZooBank LSIDs (Life Science Identifiers) can be resolved and the associated information viewed through any standard web browser by appending the LSID to the prefix http://zoobank.org/. The LSID for this publication is: urn:lsid:zoobank.org:pub:E728C3DD-EB85-482F-ACE6-6558E3ED5441. The online version of this work is archived and available from the following digital repositories: PeerJ, PubMed Central and CLOCKSS.

Institutional abbreviations

MNHN, Muséum national d'Histoire naturelle, Paris, France; MUHNAC, Museu Nacional de História Natural e da Ciência, Lisbon, Portugal; NMR, Natuurhistorisch Museum Rotterdam, the Netherlands; OU, Geology Museum, University of Otago, Dunedin, New Zealand; UCMP, University of California Museum of Paleontology, Berkeley, USA; USNM, National Museum of Natural History, Smithsonian Institution, Washington, District of Columbia, USA; ZMT, Fossil mammals catalogue, Canterbury Museum, Christchurch, New Zealand.

RESULTS

Systematic palaeontology

Cetacea Brisson, 1762

Chaeomysticeti Mitchell, 1989

Mysticeti Gray, 1864

Cetotheriidae Brandt, 1872; *sensu* Fordyce and Marx, 2013

Metopocetus Cope, 1896

Type species. *Metopocetus durinasus* Cope, 1896

Emended diagnosis. Small to medium-sized cetotheriid differing from all other chaeomysticetes except cetotheriids in having a distally expanded compound posterior process of the

tympanoperiotic bearing a floored facial sulcus, as well as medially convergent ascending processes of the maxillae bearing an enlarged, primary dorsal infraorbital foramen [new term]; further differs from all other chaeomysticetes except cetotheriids and balaenopterids in having the ascending process of the maxilla and the parietal overlap anteroposteriorly; and from balaenopterids in having the apex of the supraoccipital shield located posterior to the supraorbital process of the frontal. Differs from other cetotheriids, including neobalaenines, in lacking a well-developed lateral tuberosity of the periotic, and in having a better-defined mallear fossa and a well-developed paroccipital concavity and tympanohyal; from all other cetotheres, except possibly *Joumocetus* Kimura and Hasegawa, 2010, in having a distinctly triangular ascending process of the maxilla; from *Herpetocetus*, *Nannocetus*, *Cephalotropis* Cope, 1896 and neobalaenines in having the posterior portion of the zygomatic process of the squamosal offset from the lateral border of the exoccipital by a distinct angle; from *Herpetocetus*, *Nannocetus* and *Piscobalaena* Pilleri and Siber, 1989 in the presence of a squamosal cleft; from *Herpetocetus* and *Nannocetus* in having a smaller temporal exposure of the alisphenoid and in having a transversely oriented postglenoid process; from *Brandtocetus* Gol'din and Startsev, 2014, *Cetotherium*, *Joumocetus*, *Kurdalagonus* Tarasenko and Lopatin, 2012, "*Aulocetus*" *latus*, "*Cetotherium*" *megalophysum,* "*Metopocetus*" *vandelli* and likely also *Herentalia* Bisconti, 2014 in having a (slightly) more plug-like compound posterior process of the tympanoperiotic; from *Brandtocetus*, *Cephalotropis*, *Cetotherium*, *Joumocetus*, *Kurdalagonus*, *Vampalus* Tarasenko and Lopatin, 2012, *Zygiocetus* Tarasenko, 2014, "*Aulocetus*" *latus*, "*Cetotherium*" *megalophysum* and "*Metopocetus*" *vandelli* in having a more rounded apex of the supraoccipital shield; from *Brandtocetus*, *Cetotherium* and *Zygiocetus* in having a tympanic bulla that is not transversely wider anteriorly than it is posteriorly; and from *Joumocetus* and *Cephalotropis* in having the parietal almost excluded from the intertemporal region.

Metopocetus hunteri, sp. nov.

Figures 2–8

LSID. urn:lsid:zoobank.org:act:391CF6D9-138C-4F88-AC4B-9903DA433FDA

Holotype. NMR 9991-07729, a partial cranium preserving the vertex, palatines, the right half of the braincase and basicranium, and the right periotic and tympanic bulla.

Locality and horizon. Sand pit at Liessel, Deurne, North Brabant, the Netherlands (Fig. 1). The coordinates of the type locality are N51°25'44" E5°49'47". The specimen was retrieved from deposits assigned to the Breda Formation, a shallow marine unit consisting of glauconiferous sands, sandy clays and clays. The Breda Formation is widespread throughout the Netherlands and comprises the greater part of the Dutch Miocene succession (Burdigalian–Tortonian), reaching as much as 700 m in thickness in some locations (Munsterman & Brinkhuis 2004).

The preservation of the dinoflagellate cyst assemblage recovered from the matrix associated with the specimen is moderate to good. In total, we recorded 28 dinoflagellate cyst species and three acritarchs (Supplementary Table 1), the most important of which include *Barssidinium taxandrianum* Louwye, 1999, *Gramocysta verricula* (Piasecki, 1980), *Habibacysta tectata* Head et al., 1989, *Hystrichosphaeropsis obscura* Habib, 1972 and *Labyrinthodinium truncatum* Piasecki, 1980. *H. tectata* first occurs in the North Atlantic realm (Porcupine Basin, off southwest Ireland) during the Langhian, around 14.2 Ma (Hilgen et al. 2012; Louwye et al. 2008; Quaijtaal et al. 2014), thus setting a maximum age for the sample. Conversely, the minimum age is determined by the highest occurrences of *Hy. obscura* and *L. truncatum* at approximately 7.6 Ma (de Verteuil & Norris 1996; Dybkjær & Piasecki 2010; Köthe 2012; Louwye & de Schepper 2010; Munsterman & Brinkhuis 2004).

The sample belongs to the late Tortonian (Late Miocene) SNSM14 Zone defined in the Netherlands (Munsterman & Brinkhuis 2004), which is equivalent to the *Hystrichosphaeropsis obscura* biozone of Denmark (Dybkjær & Piasecki 2010), and the DN9 Zone of the eastern USA and Germany (de Verteuil & Norris 1996; Köthe 2012), dated to ca 8.8–7.6 Ma (Dybkjær & Piasecki 2010). The upper boundary of the SNSM14 Zone is defined by the highest occurrence of *L. truncatum*, while the lower boundary is defined by highest occurrence of *Cleistosphaeridium placacanthum* Deflandre and Cookson, 1955, a distinctive dinoflagellate cyst species not recorded in our sample. Diagnostic species present in this zone are *G. verricula* and *Hy. obscura* (Munsterman & Brinkhuis 2004). Further evidence for this age assessment comes from the occurrence of *B. taxandrianum*, which is a rare species with a restricted occurrence in the Late Miocene of the southern North Sea Basin, including the Tortonian Diest and the latest Tortonian-Messinian Kasterlee Formations (Louwye 1999; Louwye & de Schepper 2010;

Louwye et al. 2007; Louwye & Laga 2008). This species has never been recorded from Pliocene deposits.

Besides age determination, the recovered dinoflagellates also provide some insights into the depositional environment. In this context, the presence of *Gramocysta verricula* is particularly notable. This species was first recorded from the Late Miocene Gram Formation of Denmark, where it dominates the eponymous biozone (Piasecki 1980). The latter is furthermore characterised by the disappearance of neritic genera, such as *Achomosphaera* Evitt, 1963 and *Tectatodinium* Wall, 1967, and an overall reduction in the abundance of other dinocyst species. Together, these events likely reflect a marine regression, accompanied by high sedimentation rates and an enhanced influx of freshwater (Piasecki 1980). The preference of *G. verricula* for marginal marine environments is further corroborated by its occurrence in the shallow marine Kasterlee Formation and other deposits recording marked drops in sea level (Louwye et al. 2007).

Etymology. Named after the famous Scottish surgeon and anatomist John Hunter, who was maybe the first person to recognise and write about the similarity of whales and artiodactyls (Hunter 1787).

Diagnosis. Differs from *Metopocetus durinasus* in having a somewhat narrower, less distally exposed compound posterior process of the tympanoperiotic, a less anteriorly bulging temporal wall of the squamosal and a more proximally located primary dorsal infraorbital foramen on the ascending process of the maxilla (located either more distally or absent in *M. durinasus*), as well as in lacking ankylosed nasals.

Description

Overview. The preserved, mostly right portion of the cranium lacks both the rostrum and the supraorbital process of the frontal (Fig. 2). The apex of the zygomatic process, the central portion of the nuchal crest, the tip of the postglenoid process and much of the right pterygoid are broken. The state of preservation of the bones that remain is relatively good, but a certain degree of surface damage and small pockets of remaining matrix (e.g. on the dorsal surface of the periotic)

sometimes make it difficult to discern details. Measurements of the cranium are shown in Table 1.

Maxilla, premaxilla and nasal. Of the maxilla, only the triangular ascending process is preserved, which extends posteriorly beyond the base of the supraorbital process of the frontal and overlaps with the parietal (Figs 2, 3). In cross section, the ascending process is markedly concave, with its medial border rising towards the nasal. Medially, the apices of the ascending processes are clearly convergent, but remain separated from each other by the well-developed nasals. Near the base of the ascending process, there is a large primary dorsal infraorbital foramen [new term], which is also found in other cetotheriids and exits into a short, dorsomedially oriented sulcus (Fig. 3b). Anteromedial to this foramen, there are two elongate sulci without obvious foramina running parallel to the medial margin of the maxilla. Inside the narial fossa, the maxilla gives rise to a narrow shelf supporting the anterolateral corner of the nasal.

Nothing remains of the premaxilla, but the close juxtaposition of the posterior portions of the nasals and maxillae suggests that it did not extend as far posteriorly as the other rostral bones; instead, it likely terminated somewhere along the anterior half of the nasal, as in *Herpetocetus* and, presumably, *Piscobalaena*, *"Cetotherium" megalophysum and "Metopocetus" vandelli* (El Adli et al. 2014). In dorsal view, the nasal is anteroposteriorly elongate and somewhat triangular, with its lateral and medial borders converging posteriorly (Fig. 3b). Although transversely narrow posteriorly, it is exposed on the cranial vertex along its entire length – unlike in *Herpetocetus* and *Piscobalaena*, in which the posterior portion of the nasal is nearly invisible. The anterior portions of both nasals are eroded, but seem to have formed a straight or slightly convex anterior border, without any obvious sagittal crest or anterior projection as in *Herpetocetus*, *Piscobalaena* and neobalaenines.

Frontal. Only the portion of the frontal supporting the ascending process of the maxilla is preserved (Fig. 2). In dorsal view, the frontal is almost entirely excluded from the cranial vertex by the maxilla, but still overrides much of the anterior portion of the parietal. Laterally, the posterior margin of the frontal gradually descends anteroventrally towards the base of the supraorbital process of the frontal. In lateral view, the dorsal portion of the fronto-parietal suture

is elevated into a ridge slightly overhanging the anteriormost portion of the parietal (Fig. 3a), as also seen in *Herentalia* and *Piscobalaena*.

Parietal. In dorsal view, the parietal is exposed as a thin band on the vertex, anterior to the apex of the supraoccipital shield (Fig. 3b). Anteroventral to the vertex, the parietal becomes markedly concave as it descends towards the base of the supraorbital process of the frontal. In lateral view, the parietal is slightly longer anteroposteriorly than high dorsoventrally (Fig. 4a). The parieto-squamosal suture is smooth, with no obvious hint of a ridge-like eminence or a tubercle at the point where the suture meets the nuchal crest. Unlike in *Herpetocetus*, there is no postparietal foramen (Fig. 3a).

Alisphenoid. The alisphenoid is exposed in the temporal fossa and contacts the parietal, the squamosal and the pterygoid. In lateral view, the preserved portion of the alisphenoid is nearly circular in outline and relatively large (Fig. 3a) – larger than in *Cetotherium riabinini* and comparable to that of *"Cetotherium" megalophysum*, but still much smaller than in *Herpetocetus* (El Adli et al. 2014; Gol'din et al. 2014). Anteroventrally, the alisphenoid likely contributed to the rim of the orbital fissure. In ventral view, the alisphenoid is covered by the dorsal lamina of the pterygoid.

Squamosal. In dorsal view, the temporal surface of the squamosal is relatively even and does not markedly bulge into the temporal fossa. The posterior border of the temporal fossa is smooth with no squamosal crease (Fig. 2a). There is a well-developed squamosal cleft that originates at the parieto-squamosal suture and runs towards the base of the zygomatic process (Fig. 3a); a similar cleft occurs in *Cephalotropis* and *"Cetotherium" megalophysum*. The squamosal fossa is anteroposteriorly elongate, with its floor being convex anteriorly, but concave posteriorly as it approaches the posterior apex of the nuchal crest. The zygomatic process is broken, but has a robust base bearing a distinct supramastoid crest and, unlike *Piscobalaena, "Cetotherium" megalophysum* and herpetocetines, a small squamosal prominence (Fig. 2b). Judging from what remains, the zygomatic process seems to have been oriented anteriorly. Posteriorly, the zygomatic process is laterally offset from the rest of the cranium (unlike in herpetocetines and *Caperea*), with its posterior border forming a 90 degree angle with the lateral margin of the exoccipital and the portion of the squamosal surrounding the periotic (Fig. 2a).

In lateral view, there is a well-defined sternomastoid fossa (*sensu* Bouetel & de Muizon 2006) located just ventral to the supramastoid crest (Figs 2b, 4a). The preserved portion of the postglenoid process is triangular in outline and points slightly posteroventrally. The base of the zygomatic process is robust. In posterior view, the postglenoid is parabolic in outline and seems to point directly ventrally, rather than medially as in herpetocetines, although its exact shape it lost owing to breakage (Fig. 4b). The posterior meatal crest extends from the external acoustic meatus on to the posterior face of the postglenoid process, where it forms well-developed horizontal shelf. In doing so, it defines a deep sulcus running parallel to the meatus, immediately below the sternomastoid fossa (Figs 2b, 4b).

In ventral view, the falciform process of the squamosal is robust, distinctly squared and, along with adjacent portions of the squamosal, forms virtually the entire rim of the foramen pseudovale (Fig. 5). The external acoustic meatus is relatively broad, with its roof – the posterior meatal crest – extending on to the anterior face of the posterior process of the periotic. Together with the falciform process, the innermost portion of the internal acoustic meatus defines a strikingly rectangular window exposing the lateral surface of the anterior process of the periotic (Fig. 6a). Anterior to the meatus, the postglenoid process of the squamosal is thin anteroposteriorly, oriented transversely and medially confluent with the anterior meatal crest.

Supraoccipital. In dorsal view, the supraoccipital shield is broadly triangular, with a straight to slightly convex lateral border (= nuchal crest) and a rounded apex (Fig. 2a). As in all other cetotheriids except neobalaenines, the nuchal crest is oriented mostly dorsally and does not overhang the temporal fossa. Just posterior to the apex of the supraoccipital shield, there is a relatively broad, tabular area that posteriorly gives rise to an external occipital crest. The latter is well-developed and extends along at least one third of the dorsal surface of the supraoccipital; further posteriorly, the central portion of the bone is missing (Fig. 2). In posterior view, the supraoccipital is markedly concave transversely, without any obvious tubercles on either side of the external occipital crest (Fig. 4b).

Exoccipital and basioccipital. In dorsal view, the exoccipital is well developed and extends posteriorly both beyond the level of the occipital condyle and the posterior apex of the nuchal crest (Fig. 2). The occipital condyle is large and situated on a distinct neck. In posterior view, the paroccipital process is squared in outline and extends ventrally to roughly the same level as the

basioccipital crest (Fig. 4b). Medial to the paroccipital process, the jugular notch is narrow transversely and elongate dorsoventrally. The foramen magnum is framed by the dorsal portion of the occipital condyle.

In ventral view, the entire ventral surface of the exoccipital is excavated by the paroccipital concavity (Fig. 6a). Medially, this fossa invades, and is thus partially floored by, the ventromedial corner of the paroccipital process, which also separates it from the jugular notch. Laterally, the paroccipital concavity is relatively open. Anteriorly, the floor of the paroccipital concavity forms a shelf that partially floors the facial sulcus, and is in turn underlapped by a posteroventral flange [new term] arising from the compound posterior process of the tympanoperiotic (Fig. 6a, c). This contact between the exoccipital and the posteroventral flange of the tympanoperiotic – which, to our knowledge, is unique among mysticetes – creates a continuous bony surface that allows the paroccipital concavity to extend far on to the tympanoperiotic itself (Figs 5, 6a, c). Medial to the well-marked jugular notch, the basioccipital crest is transversely broad, triangular and oriented anteroposteriorly (Fig. 5). As far as can be told, the suture between the basioccipital and the basisphenoid is ventrally covered by the posteriormost portion of the vomer.

Vomer. Only the posterior portion of the vomer is preserved. In the basicranium, the vomer is broadly exposed posterior to what remains of the choanae and overrides much of the medial lamina of the pterygoid. Further anteriorly, the vomer is exposed between the anterior portions of the palatines, as in all other cetotheriids for which the condition of this part of the vomer is known (Fig. 5).

Palatine. Both palatines are preserved, but have lost nearly all of their outer margins; they are markedly concave transversely, as if pinched, thus forming a distinct ventral keel. A similar condition occurs in *Cephalotropis*, *Caperea* and to some degree *Herpetocetus*. By contrast, the palatines are only slightly concave in *Piscobalaena*, *"Cetotherium" megalophysum* and *"Metopocetus" vandelli* , and seemingly flattened or even slightly convex in *Cetotherium* (Gol'din et al. 2014).

Pterygoid. The ventral portion of the pterygoid is mostly missing, except for a small portion contributing to the rim of the foramen pseudovale. Dorsally, the pterygoid roofs almost the entire

pterygoid sinus fossa, which extends anteriorly approximately to the level of the foramen pseudovale. Posteriorly, the dorsal or lateral lamina of the pterygoid overrides the anteriormost portion of the anterior process of the periotic (Figs 5, 6a). Medially, the pterygoid is continuous with the basioccipital crest.

Periotic, stapes and tympanohyal. In ventral view, the anterior process of the periotic appears to be transversely thickened, but not hypertrophied (Fig. 6a). The lateral tuberosity is indistinct, in stark contrast to herpetocetines and, to a lesser degree, *Brandtocetus* and *Kurdalagonus*. The anterior pedicle is relatively small and located just anterior to the broad and comparatively well-defined mallear fossa. There is no anterior bullar facet, and seemingly no distinct ridge for the attachment of the tensor tympani muscle, unlike in herpetocetines and *Piscobalaena*. The pars cochlearis is rounded and posteriorly terminates in an elongate caudal tympanic process which approaches, but does not contact, the crista parotica (Fig. 6b). The presence or absence of the promontorial groove is unclear. Sediment obscures both the distal opening of the facial canal and the fenestra ovalis, but the ventral portion of the right stapes can be seen to protrude from the latter.

The compound posterior process of the tympanoperiotic (hereafter shortened to posterior process) is oriented posterolaterally relative to the anteroposterior axis of the pars cochlearis. At its base, it carries the posterior pedicle of the tympanic bulla, which appears curved as a result of internal excavation by the tympanic cavity (Fig. 6 a, b). Next to the posterior pedicle, there is a large, trumpet-shaped tympanohyal fused to the crista parotica (Fig. 6b). The presence of such a well-developed tympanohyal is rare among mysticetes, and among cetotheriids only occurs in *Metopocetus*. Along its anterior margin, the posterior process gives rise to a posteriorly excavated anteroventral flange [new term], which anteriorly delimits the expanded paroccipital concavity (Fig. 6a, c). The floor of the paroccipital concavity is formed by a horizontal posteroventral flange [new term] that underlaps both the facial canal and the anterior rim of the ventral surface of the exoccipital (Fig. 6a, c).

In medial view, the anterior process appears two-bladed, but its actual shape is difficult to discern because it is partially covered by the dorsal/lateral lamina of the pterygoid. The fenestra rotunda is large and offset from the posterior border of the pars cochlearis by a broad shelf (Fig. 6b). Ventrally, this shelf merges with the elongate, posteriorly oriented caudal tympanic process.

In dorsal view, the internal acoustic meatus and the proximal opening of the facial canal are comparable in size and separated by a well-developed transverse septum (Fig. 6d). Together, they are nearly, albeit not perfectly, in line with the circular aperture for the cochlear aqueduct. The aperture for the vestibular aqueduct is obscured by matrix, but does not seem to overlap anterodorsally with the aperture for the cochlear aqueduct. The suprameatal fossa is shallow with a rounded lateral border; there is no distinct superior process. In lateral view, the posterior process is broadly exposed on the lateral skull wall, but anteroposteriorly narrower than in *Metopocetus durinasus* and herpetocetines (Fig. 6c) (Whitmore & Barnes 2008). The facial canal runs along the posterior border of the posterior process. Just anterior to the facial canal, there is a deep fossa of unknown function and homology, ventrally delimited by the expanded distal portion of the anteroventral flange (Fig. 6c).

Tympanic bulla. In dorsal view, the involucrum is relatively narrow in the area of the anteroposteriorly broad Eustachian outlet, but then rapidly widens as it approaches the posterior pedicle (Fig. 7a). There are no obvious transverse sulci on its dorsal surface, except for some rims in the vicinity of the posterior pedicle. Transverse sulci are common in mysticetes and marked in adult specimens of at least some cetotheriids (e.g. *Brandtocetus chongulek* and *Herpetocetus transatlanticus*). It is possible that their absence in NMR 9991-07729 is a result of surface damage, although it seems likely that even in a perfectly preserved bulla they would have been at best faintly developed. A smooth involucrum is typical of juvenile individuals, and may hence indicate that NMR9991-07729 is more likely to be an old juvenile than an adult.

The involucral ridge (*sensu* Oishi & Hasegawa 1995) extends all the way to the medial margin of the bulla, largely as a result of the robustness of the inner posterior prominence (= medial lobe of the tympanic bulla). The sigmoid process is oriented transversely and situated roughly halfway along the anteroposterior length of the bulla; its dorsomedial corner is distinct from the anterior process of the malleus and twisted slightly posteriorly. The conical process is transversely thickened and located entirely posterior to the sigmoid process. Opposite the conical process, the posterior pedicle is located relatively close to the posterior border of the bulla and internally excavated by a branch of the tympanic cavity. In medial view, the bulla is somewhat pear-shaped in outline, with the dorsal surface of the involucrum being distinctly concave (Fig. 7b). In the region of the Eustachian outlet, the dorsal surface of the involucrum is depressed into

a broad, smooth fossa. The main and involucral ridges converge anteriorly, while being more clearly separated posteriorly by a relatively shallow median furrow and interprominential notch. On the medial face of the conical process, the tympanic sulcus follows a broad, horizontal ridge somewhat similar to that in *Piscobalaena*, before suddenly turning 90 degrees to run dorsally on to the posterior surface of the sigmoid process (Fig. 7g).

In ventral view, the anterior portion of the bulla appears to be more rounded than in most other cetotheriids, although the anterior border is still somewhat flattened (Fig. 7c). There is no anterolateral shelf. The anterolateral corner of the bulla is inflated and forms a distinct lobe anterior to the lateral furrow. The outline of the main ridge (*sensu* Oishi & Hasegawa 1995) is convex. In lateral view, the lateral furrow is distinct and oriented vertically (Fig. 7d). The sigmoid cleft ventrally merges into the outer surface of the bulla, so that there is no discernable ventral border of the sigmoid process. Consequently, the latter does not overlap the anterior portion of the conical process, although the two processes are still connected by a well-developed horizontal rim. The conical process itself is dorsally rounded, not flattened as in *Herpetocetus* and *Caperea*.

In anterior view, the ventral surface of the bulla is transversely convex, except for a small concave portion immediately medial to the main ridge (Fig. 7e). The rim of the Eustachian outlet is oriented horizontally and continuous with the dorsal surface of the involucrum. The lateral margin of the sigmoid process is oriented slightly dorsolaterally, but the process as a whole is not laterally deflected. In posterior view, the main ridge of the bulla is oriented medially, so that the inner posterior prominence faces dorsally, and the outer posterior prominence ventrally (Fig. 7f). Like most other chaeomysticetes, the bulla thus shows a marked degree of medial rotation relative to the condition in archaic toothed mysticetes and eomysticetids. The involucral ridge is well developed and terminates ventral to the base of the posterior pedicle. There is neither a transverse crest connecting the main and involucral ridges, nor an elliptical foramen. The lateral margin of conical process is straight.

Malleus. In posterodorsal view, the articular facets for the incus are oriented at right angles to each other, with the vertical facet being slightly larger (Fig. 8a). The head of the malleus is broadly rounded and separated from the tubercle by a distinct groove. In anterior view, the bottom of the head and the anterior process are excavated by the sulcus for the chorda tympani.

Adjacent to the internal margin of the head, the muscular process bears a well-defined, circular pit for the insertion of the tendon of the tensor tympani muscle (Fig. 8b).

DISCUSSION AND CONCLUSIONS

Age of *Metopocetus*

The age of the hitherto only member of *Metopocetus*, *M. durinasus*, has been a matter of some debate. In his original description of the holotype and only specimen of *M. durinasus*, USNM 8518, Cope (1896) provided little detail as to the provenance of the material , stating only that it had been collected from "a Miocene marl from near the mouth of the Potomac river" (p. 143). Subsequent authors interpreted this description of the type locality to refer to either the Calvert Formation (Kellogg 1931; Kellogg 1968) or the St. Mary's Formation (Case 1904), implying either a Langhian or a Tortonian age, respectively (Marx & Fordyce 2015). Determining which of these possibilities is correct is crucial, given that a Langhian age would make *M. durinasus* the oldest reported cetotheriid. The occurrence of *M. hunteri* in Tortonian strata of Europe suggests that *M. durinasus* may also date from this stage, especially given the relatively close morphological resemblance of the two species. This idea is furthermore consistent with the occurrence of at least two other cetotheriids (*Cephalotropis coronatus* and "*Cetotherium*" *megalophysum*) in the St Mary's Formation, whereas the family is conspicuously absent from the Calvert Formation. Pending the discovery of additional specimens and/or direct dating evidence, we thus suggest that *M. durinasus* should likely be regarded as Tortonian.

Ontogenetic age

Except for those of the maxillae and nasals, all of the cranial sutures are closed, which suggests that this individual is at or near its adult size. Support for this estimate comes from the presence of several well-developed bony crests, such as the external sagittal crest on the supraoccipital, the supramastoid crest on the squamosal and a reasonably distinct main ridge on the tympanic bulla. The anteroventral displacement of the maxillae and nasals does not necessarily contradict this assessment, as in modern mysticetes the sutures connecting these bones tend to be relatively loose even in adults to facilitate rostral kinesis (e.g. Deméré & Berta 2008). Potentially more problematic is the rather smooth texture of the dorsal surface of the involucrum, which is typical of juveniles. Some of this smoothness may be due to superficial damage, but there is no evidence

that the original texture of the involucrum markedly differed from what is preserved. In the absence of more definitive markers of development, such as vertebral or long bone epiphyses, it thus seems most consistent to interpret the present material as a relatively old juvenile.

Phylogeny

Our phylogenetic analysis (average deviation of split frequencies 0.016 after 50 million generations) clearly places *Metopocetus hunteri* inside both Cetotheriidae and as sister to *M. durinasus* (Fig. 9). "*Metopocetus*" *vandelli* is not closely related to either *M. durinasus* or *M. hunteri*, and instead clusters with "*Aulocetus*" *latus* and "*Cetotherium*" *megalophysum*. Beyond this, our results largely correspond to those of Marx and Fordyce (2015), but differ in two important aspects: (1) *Metopocetus* is no longer grouped with *Piscobalaena* and "*C.*" *megalophysum*, and instead now forms part of a basal lineage along with *Cephalotropis*; (2) *Piscobalaena* and "*C.*" *megalophysum* no longer cluster with *Cetotherium* and instead now form a clade with Herpetocetinae + Neobalaeninae.

Cephalotropis has previously been found to occupy a basal position within Cetotheriidae (El Adli et al. 2014; Gol'din & Steeman 2015), which is at least partially reflected by our results. Nevertheless, the grouping of *Metopocetus* and *Cephalotropis* is novel and somewhat surprising, given their superficially rather different morphologies. This discrepancy is reflected in the low posterior probability (<50%) of the node that unites them, as well as the considerable length of the branch leading to *Cephalotropis*. The clade is supported by the presence of a well-developed median keel on the palatines (char. 22), but it is worthwhile noting that a similar morphology also occurs in neobalaenines and, up to a point, *Herpetocetus*.

The move of *Piscobalaena* closer to herpetocetines is less controversial than the grouping of *Cephalotropis* and *Metopocetus*, and brings our findings into line with those of several earlier studies (Bisconti 2015; El Adli et al. 2014; Gol'din & Startsev 2014; Gol'din & Steeman 2015). Nevertheless, the branch uniting *Piscobalaena* +*"Cetotherium" megalophysum* with herpetocetines + neobalaenines has a low posterior probability, even though it is supported by 3 synapomorphies: an orbitotemporal crest running close to the posterior border of the supraorbital process (char. 80); absence of the squamosal prominence (char. 106); and presence of a sulcus marking the attachment of the mylohyoid muscle on the inside of the mandible (char. 238).

Considerably better supported relationships, though not of immediate interest to this study, include the clade comprising the *Cetotherium*-like taxa (*Brandtocetus*, *Cetotherium* and *Kurdalagonus*) from the Eastern Paratethys, neobalaenines, herpetocetines, and the branch uniting the latter two (Fig. 9).

The relatively basal position of *Metopocetus* is inconsistent with it showing a morphology truly intermediate between that of herpetocetines and other cetotheriids (Whitmore & Barnes 2008). It furthermore implies that the pronounced widening of the distal portion of the compound posterior process – a hallmark of cetotheres – may have occurred more than once. The posterior process of *all* cetotheriids is large relative to that of most other mysticetes, but there are clear differences in scale: its distal end is most expanded in herpetocetines, neobalaenines, *Cephalotropis*, *M. durinasus* and *Piscobalaena*; somewhat less so in *Brandtocetus*, *Cetotherium*, *Kurdalagonus*, *M. hunteri* and *Zygiocetus*; and even less so in *"Aulocetus" latus*, "*C.*" *megalophysum* and "*M.*" *vandelli*.

"Cetotherium" megalophysum and "*Metopocetus*" *vandelli*. were included in Herpetocetinae as sister to *Nannocetus* by El Adli et al. (2014), whereas "*C.*" *megalophysum* fell out as sister to *Piscobalaena* in the present analysis. Both topologies require that the distal widening of the posterior process either occurred in parallel in several lineages, or else was later reduced in certain species. The topology of Gol'din and Steeman (2015) partially circumvents this problem by excluding "*C.*" *megalophysum* and "*M.*" *vandelli* from Cetotheriidae altogether, but even in this case widening of the posterior process would have occurred at least twice: once in the lineage leading to *Cephalotropis* and neobalaenines, and once with their Cetotheriidae proper. There is, of course, a distinct possibility that this patchy character distribution is simply the result of errors in the cladistic hypotheses. Nevertheless, given the wide range of morphologies and generally mosaic distribution of characters within Cetotheriidae, we suggest that the presence of an expanded posterior process may reflect a shared evolutionary trend within the family, rather than a definitive uniting character. A better understanding of the history of this unique feature will likely depend on getting to grips with its function first.

In addition to that of *M. hunteri*, the position of "*Metopocetus*" *vandelli* is of particular interest to the present study, as it is the only other species ever referred to *Metopocetus* (Kellogg 1941). Recent analyses have cast considerable doubt on this assignment, and variously grouped

"*M.*" *vandelli* with *"C." megalophysum*, a clade comprising *Piscobalaena*, *Metopocetus* and herpetocetines, or even included it in a different family, Tranatocetidae, thought to be related to balaenopterids and eschrichtiids (El Adli et al. 2014; Gol'din & Startsev 2014; Gol'din & Steeman 2015). Even at a relatively cursory glance, "*M.*" *vandelli* clearly differs from both *M. durinasus* and *M. hunteri* in a range of features, including (1) a more elongate, finger-like ascending process of the maxilla; (2) a more pointed, dorsally flattened supraoccipital shield lacking a well-developed external occipital crest; (3) the apparent absence of a squamosal cleft (not completely clear owing to incomplete preparation of the type specimen); (4) comparatively flat palatines not forming a medial ridge; (5) a markedly less expanded distal portion of the compound posterior process (to be confirmed by further preparation); and (6) a more gracile exoccipital (Fig. 10). Taken together, these differences speak against any particularly close affinity of "*M.*" *vandelli* with *Metopocetus* and thus support its removal from this genus, as advocated by several other recent studies (El Adli et al. 2014; Gol'din & Startsev 2014; Gol'din & Steeman 2015; Whitmore & Barnes 2008).

Our analysis agrees with other recent studies in grouping *"A." latus* and *"M." vandelli* into a clade with *"C." megalophysum* (El Adli et al. 2014; Gol'din & Steeman 2015). Support for this branch is reasonable at 89%, although we currently only recognise a single synapomorphy: the posterior projection of the occipital condyles beyond the level of the exoccipitals (char. 139). A more detailed examination of this proposed relationship is beyond the scope of this study, and furthermore currently hampered by the incomplete state of preparation or lack of description of the available material. Nevertheless, in light of the consistency with which these taxa have been grouped together in recent analyses, we tentatively suggest that all of them may not only be closely related, but possibly even congeneric or conspecific. Further data, especially on the morphology of the ear bones, will provide the means to test this idea.

Paroccipital concavity

Metopocetus stands out for having an unusually enlarged paroccipital concavity extending across both the exoccipital and the compound posterior process of the tympanoperiotic (Fig. 6a). A fossa excavating the anteroventral surface of the paroccipital process occurs in a variety of cetaceans, including archaeocetes, mysticetes and odontocetes (e.g. Deméré & Berta 2008; Fraser & Purves 1960; Martínez Cáceres & de Muizon 2011). Among mysticetes, the

paroccipital concavity tends to be best developed in archaic forms and least in the extant taxa (e.g. Deméré & Berta 2008; El Adli et al. 2014). Nevertheless, its size and shape is variable, and the concavity remains well-developed in at least one living species, the grey whale, *Eschrichtius robustus* (Lilljeborg, 1861) (Fig. 11). In terms of its function, the paroccipital concavity is generally interpreted as the bony correlate of the posterior sinus and/or the site of the ligamentous attachment of the stylohyal to the basicranium (Beauregard 1894; Boessenecker & Fordyce 2015; Bouetel & de Muizon 2006; Deméré & Berta 2008; El Adli et al. 2014; Fraser & Purves 1960; Oelschläger 1986). Unfortunately, little has been published on either of these features in mysticetes, which makes it difficult to draw any firm conclusions.

Fraser and Purves (1960: plates 6 and 7) show the small posterior sinus of extant *Caperea marginata* and *Balaenoptera acutorostrata* as occupying only a fraction of what remains of the paroccipital concavity in these taxa. If correct, then this would imply that the sinus cannot by itself account for the development of the paroccipital concavity as a whole. However, it needs to be noted that their assessment was largely based on the interpretation of osteological correlates and a previous description of *B. acutorostrata* (without any figures providing a detailed view of the posterior sinus) by Beauregard (1894), and hence may not be completely accurate. The ligamentous attachment of the stylohyal to the exoccipital in cetaceans has long been noted (Flower 1885), and an enlargement of this structure seems particularly plausible in the case of *Metopocetus* with its well-developed tympanohyal. Nevertheless, it remains questionable whether the ligament would have filled the entire space defined by the paroccipital concavity. Additional data on the anatomy of this region in extant cetaceans are needed to determine what usually fills the paroccipital concavity in mysticetes, and thus ultimately what may have triggered it to grow so large in *Metopocetus*.

Primary dorsal infraorbital foramen

All cetotheriids except neobalaenines and, perhaps, *Cephalotropis*, share the presence of an often enlarged, primary dorsal infraorbital foramen situated close to the base of the ascending process of the maxilla (e.g. Bouetel & de Muizon 2006; El Adli et al. 2014; Gol'din et al. 2014; Kimura & Hasegawa 2010) (Fig. 12). In some taxa, such as *Herpetocetus*, and, possibly, *Herentalia*, a secondary foramen may also be present (Bisconti 2015; Boessenecker 2013; El Adli et al. 2014). Posteriorly, the foramen (or foramina) opens into a sulcus of variable length, which generally

runs dorsally along the ascending process of the maxilla towards the cranial vertex. While the sulcus itself may be relatively short, the ascending process of the maxilla itself is often transversely concave (e.g. in *Herentalia*, *Metopocetus*, *Piscobalaena*, and to some degree also *Herpetocetus*), suggesting that the primary dorsal infraorbital foramen may supply a larger structure ascending along the maxilla towards the top of the cranium.

Many mysticetes besides cetotheriids, including extant balaenids and balaenopterids, also possess what appears to be the homologue (or homologues) of the primary dorsal infraorbital foramen of cetotheriids; however, in these taxa the development of the foramen is often not as pronounced, often not accompanied by distinct sulci, and not as consistent (e.g. the foramen appears to be variable in *Balaena mysticetus* Linnaeus, 1758 and completely absent in *Balaenella brachyrhynus* Bisconti, 2005). The function of the primary dorsal infraorbital foramen is not entirely clear, especially in light of the fact that, at least in cetotheriids, it opens posterior to the level of the anterior border of the nasals (Fig. 12), and thus presumably cannot supply the nasal apparatus. Given the size of the foramen, as well as its consistent occurrence and the size and direction of the associated sulci (e.g. in *Piscobalaena nana*), it is tempting to speculate that the distinctive pattern of cetotheriid facial telescoping (i.e. posteriorly convergent maxillae resulting in shortened premaxillae and transversely compressed nasals) may at least partially have been driven by whatever soft tissue structure the foramen correlates with. Additional data on the function of the primary dorsal infraorbital foramen in living species may help to test this hypothesis.

ACKNOWLEDGEMENTS

We thank Klaas Post for donating the specimen and allowing us to study it; Robert W. Boessenecker, Mark. D. Uhen, Thomas A. Deméré and the editor Nicholas Pyenson for their helpful and constructive comments on the manuscript; R. Ewan Fordyce for insightful discussions and providing the photograph of *Metopocetus durinasus*; Seraina Klopfstein for technical advice on the total evidence analysis; Carl Buell for providing illustrative drawings of living and fossil cetaceans; and the staff of all of the institutions involved for access to material and help during our visits.

609

610 References

611 Antunes MT, Legoinha P, Cunha PP, and Pais J. 2000. High resolution stratigraphy and miocene facies
612 correlation in Lisbon and Setúbal Peninsula (Lower Tagus basin, Portugal). *Ciências da Terra*
613 14:183-190.

614 Beauregard H. 1894. Recherches sur l'appareil auditif chez les mammifères III. *Journal de l'Anatomie et*
615 *de la Physiologie* 30:366-413.

616 Bisconti M. 2015. Anatomy of a new cetotheriid genus and species from the Miocene of Herentals,
617 Belgium, and the phylogenetic and palaeobiogeographical relationships of Cetotheriidae s.s.
618 (Mammalia, Cetacea, Mysticeti). *Journal of Systematic Palaeontology* 13:377-395.

619 Boessenecker RW. 2013. Pleistocene survival of an archaic dwarf baleen whale (Mysticeti:
620 Cetotheriidae). *Naturwissenschaften* 100:365-371.

621 Boessenecker RW, and Fordyce RE. 2015. A new eomysticetid (Mammalia: Cetacea) from the Late
622 Oligocene of New Zealand and a re-evaluation of '*Mauicetus*' *waitakiensis*. *Papers in*
623 *Palaeontology* 1:107-140.

624 Bouetel V, and de Muizon C. 2006. The anatomy and relationships of *Piscobalaena nana* (Cetacea,
625 Mysticeti), a Cetotheriidae s.s. from the early Pliocene of Peru. *Geodiversitas* 28:319-395.

626 Brandt JF. 1873. Untersuchungen über die fossilen und subfossilen Cetaceen Europa's. *Mémoires de*
627 *l'Académie impériale des sciences de St-Pétersbourg* 20:1-371.

628 Case EC. 1904. Mammalia. In: Clark WB, ed. *Miocene*. Baltimore: The John Hopkins Press, 3-57.

629 Cope ED. 1896. Sixth contribution to the knowledge of the Miocene fauna of North Carolina.
630 *Proceedings of the American Philosophical Society* 35:139–146.

631 de Verteuil L, and Norris G. 1996. Miocene dinoflagellate stratigraphy and systematics of Maryland and
632 Virginia. *Micropaleontology* 42 (Suppl.):1-172.

633 Deméré TA, and Berta A. 2008. Skull anatomy of the Oligocene toothed mysticete *Aetioceus weltoni*
634 (Mammalia; Cetacea): Implications for mysticete evolution and functional anatomy. *Zoological*
635 *Journal of the Linnean Society* 154:308-352.

636 Deméré TA, McGowen MR, Berta A, and Gatesy J. 2008. Morphological and molecular evidence for a
637 stepwise evolutionary transition from teeth to baleen in mysticete whales. *Systematic Biology*
638 57:15-37.

639 Dybkjær K, and Piasecki S. 2010. Neogene dinocyst zonation for the eastern North Sea Basin, Denmark.
640 *Review of Palaeobotany and Palynology* 161:1-29.
641 El Adli JJ, Deméré TA, and Boessenecker RW. 2014. *Herpetocetus morrowi* (Cetacea: Mysticeti), a new
642 species of diminutive baleen whale from the Upper Pliocene (Piacenzian) of California, USA, with
643 observations on the evolution and relationships of the Cetotheriidae. *Zoological Journal of the*
644 *Linnean Society* 170:400-466.
645 Estevens M, and Antunes MT. 2004. Fragmentary remains of odontocetes (Cetacea, Mammalia) from
646 the Miocene of the Lower Tagus Basin (Portugal). *Revista Espanola de Paleontologia* 19:93-108.
647 Fensome RA, MacRae RA, and Williams GL. 2008. DINOFLAJ2, Version 1. Data Series no 1: American
648 Association of Stratigraphic Palynologists. p 937.
649 Flower WH. 1885. *An Introduction to the Osteology of the Mammalia*. London: Macmillan and Co.
650 Fordyce RE, and Marx FG. 2013. The pygmy right whale *Caperea marginata*: the last of the cetotheres.
651 *Proceedings of the Royal Society B* 280:20122645.
652 Fraser FC, and Purves PE. 1960. Hearing in cetaceans. *Bulletin of the British Museum (Natural History)*
653 *Zoology* 7:3-139.
654 Gol'din P, and Startsev D. 2014. *Brandtocetus*, a new genus of baleen whales (Cetacea, Cetotheriidae)
655 from the Late Miocene of Crimea, Ukraine. *Journal of Vertebrate Paleontology* 34:419-433.
656 Gol'din P, Startsev D, and Krakhmalnaya T. 2014. The anatomy of the Late Miocene baleen whale
657 *Cetotherium riabinini* from Ukraine. *Acta Palaeontologica Polonica* 59:795-814.
658 Gol'din P, and Steeman ME. 2015. From problem taxa to problem solver: a new Miocene family,
659 Tranatocetidae, brings perspective on baleen whale evolution. *PLoS ONE* 10:e0135500.
660 Hilgen FJ, Lourens LJ, and Van Dam JA. 2012. The Neogene Period. In: Gradstein FM, Ogg JG, Schmitz M,
661 and Ogg G, eds. *The Geologic Time Scale 2012*. Oxford: Elsevier, 923–978.
662 Hunter J. 1787. Observations on the structure and oeconomy of whales. *Philosophical Transactions of*
663 *the Royal Society of London B* 77:371-450.
664 Kellogg R. 1931. Pelagic mammals of the Temblor Formation of the Kern River region, California.
665 *Proceedings of the California Academy of Sciences* 19:217-397.
666 Kellogg R. 1941. On the cetotheres figured by Vandelli. *Boletim do Museu e Laboratório Mineralógico e*
667 *Geológico da Faculdade de Ciências da Universidade de Lisboa* 7-8:13-23.
668 Kellogg R. 1968. Fossil marine mammals from the Miocene Calvert Formation of Maryland and Virginia,
669 part 5: Miocene Calvert mysticetes described by Cope. *United States National Museum Bulletin*
670 247:103-132.

671 Kimura T, and Hasegawa Y. 2010. A new baleen whale (Mysticeti: Cetotheriidae) from the earliest late
672 Miocene of Japan and a reconsideration of the phylogeny of cetotheres. *Journal of Vertebrate*
673 *Paleontology* 30:577-591.
674 Köthe A. 2012. A revised Cenozoic dinoflagellate cyst and calcareous nannoplankton zonation for the
675 German sector of the southeastern North Sea Basin. *Newsletters on Stratigraphy* 45:189-220.
676 Louwye S. 1999. New species of organic-walled dinoflagellates and acritarchs from the Upper Miocene
677 Diest Formation, northern Belgium (southern North Sea Basin). *Review of Palaeobotany and*
678 *Palynology* 107:109-123.
679 Louwye S, and de Schepper S. 2010. The Miocene–Pliocene hiatus in the southern North Sea Basin
680 (northern Belgium) revealed by dinoflagellate cysts. *Geological Magazine* 147:760-776.
681 Louwye S, de Schepper S, Laga P, and Vandenberghe N. 2007. The Upper Miocene of the southern North
682 Sea Basin (northern Belgium): a palaeoenvironmental and stratigraphical reconstruction using
683 dinoflagellate cysts. *Geological Magazine* 144:33-52.
684 Louwye S, Foubert A, Mertens K, and van Rooij D. 2008. Integrated stratigraphy and palaeoecology of
685 the Lower and Middle Miocene of the Porcupine Basin. *Geological Magazine* 145:321-344.
686 Louwye S, and Laga P. 2008. Dinoflagellate cyst stratigraphy and palaeoenvironment of the marginal
687 marine Middle and Upper Miocene of the eastern Campine area, northern Belgium (southern
688 North Sea Basin). *Geological Journal* 43:75-94.
689 Martínez Cáceres M, and de Muizon C. 2011. A new basilosaurid (Cetacea, Pelagiceti) from the Late
690 Eocene to Early Oligocene Otuma Formation of Peru. *Comptes Rendus Palevol* 10:517-526.
691 Marx FG, Buono MR, Fordyce RE, and Boessenecker RW. 2013. Juvenile morphology: a clue to the
692 origins of the most mysterious of mysticetes? *Naturwissenschaften* 100:257-261.
693 Marx FG, and Fordyce RE. 2015. Baleen boom and bust: a synthesis of mysticete phylogeny, diversity
694 and disparity. *Royal Society Open Science* 2:140434.
695 Mead JG, and Fordyce RE. 2009. The therian skull: a lexicon with emphasis on the odontocetes.
696 *Smithsonian Contributions to Zoology* 627:1-248.
697 Miller MA, Pfeiffer W, and Schwartz T. 2010. Creating the CIPRES Science Gateway for inference of large
698 phylogenetic trees. Proceedings of the Gateway Computing Environments Workshop (GCE), 14
699 Nov 2010. New Orleans. p 1-8.
700 Munsterman DK, and Brinkhuis H. 2004. A southern North Sea Miocene dinoflagellate cyst zonation.
701 *Geologie en Mijnbouw* 83:267-285.

Oelschläger HA. 1986. Comparative morphology and evolution of the otic region in toothed whales (Cetacea, Mammalia). *American Journal of Anatomy* 177:353-368.

Oishi M, and Hasegawa Y. 1995. Diversity of Pliocene mysticetes from eastern Japan. *Island Arc* 3:436-452.

Pais J, Legoinha P, and Estevens M. 2008. Património paleontológico do Concelho de Almada. In: Callapez PM, Rocha RB, Marques JF, Cunha L, and Dinis P, eds. *A Terra: Conflitos e Ordem Livro homenagem Prof António Ferreira Soares*. Coimbra: Museu Mineralógico e Geológico da Universidade de Coimbra, 143-158.

Piasecki S. 1980. Dinoflagellate cyst stratigraphy of the Miocene Hodde and Gram formations, Denmark. *Bulletin of the Geological Society of Denmark* 29:53-76.

Quaijtaal W, Donders TH, Persico D, and Louwye S. 2014. Characterising the middle Miocene Mi-events in the Eastern North Atlantic realm: A first high-resolution marine palynological record from the Porcupine Basin. *Palaeogeography, Palaeoclimatology, Palaeoecology* 399:140-159.

Steeman ME. 2007. Cladistic analysis and a revised classification of fossil and recent mysticetes. *Zoological Journal of the Linnean Society* 150:875-894.

Tarasenko KK, and Lopatin AV. 2012. New baleen whale genera (Cetacea, Mammalia) from the Miocene of the northern Caucasus and Ciscaucasia: 2. *Vampalus* gen. nov. from the Middle-Late Miocene of Chechnya and Krasnodar Region. *Paleontological Journal* 46:620-629.

Whitmore FC, Jr, and Barnes LG. 2008. The Herpetocetinae, a new subfamily of extinct baleen whales (Mammalia, Cetacea, Cetotheriidae). *Virginia Museum of Natural History Special Publication* 14:141-180.

Figure captions

Figure 1. Type locality of *Metopocetus hunteri*. Drawing of cetotheriid by Carl Buell.

Figure 2. Cranium of *Metopocetus hunteri* in (A) dorsal and (B) posterolateral view.

Figure 3. Detail of the cranium of *Metopocetus hunteri*: (A) posteromedial wall of temporal fossa in anteromedial view; (B) vertex in anterodorsal view.

Figure 4. Cranium of *Metopocetus hunteri* in (A) lateral and (B) posterior view.

730 **Figure 5.** Cranium of *Metopocetus hunteri* in ventral view.

731 **Figure 6.** Basicranium and periotic of *Metopocetus hunteri*: (A) right portion of basicranium in
732 ventral view; (B) central portion of periotic in ventromedial view; (C) compound posterior
733 process of tympanoperiotic in external view; (D) central portion of periotic in dorsal view.
734 Abbreviations: al, anterolateral; ant, anterior; dor, dorsal; fac., facial sulcus; lat, lateral; parocc.
735 conc., paroccipital concavity; pl, posterolateral; pos, posterior; post. process, compound posterior
736 process.

737 **Figure 7.** Tympanic bulla of *Metopocetus hunteri* in (A) dorsal, (B) medial, (C) ventral, (D)
738 lateral, (E) anterior, (F) posterior and (G) slightly oblique dorsomedial view. A–G, photographs;
739 A'–G' line drawings. Abbreviations: ant, anterior; dl, dorsolateral; dor, dorsal; lat, lateral; med,
740 medial; pm, posteromedial; pos, posterior.

741 **Figure 8.** Malleus of *Metopocetus hunteri* in (A) posterior and (B) anterior view. Abbreviations:
742 dor, dorsal; med, medial; ven, ventral.

743 **Figure 9.** Phylogenetic relationships of *Metopocetus hunteri*, based on a dated total evidence
744 analysis. All data except the codings for *M. hunteri* are from Marx & Fordyce (2015: fig. 2).
745 Drawings of cetaceans by Carl Buell. Abbreviations: Pli., Pliocene; Pls., Pleistocene.

746 **Figure 10.** Morphological features distinguishing "*Metopocetus*" *vandelli* from *M. durinasus* and
747 *M. hunteri*. Crania in dorsal view.

748 **Figure 11.** Left portion of the basicranium of the extant grey whale *Eschrichtius robustus*
749 (USNM 364973) in ventrolateral view, highlighting the position of the paroccipital concavity.

750 **Figure 12.** Vertex of the cetotheriids *Piscobalaena nana* (MNHN SAS1616), *Herpetocetus*
751 *morrowi* (UCMP 124950) and *"Metopocetus" vandelli* (MUHNAC A1) in dorsal view, showing
752 the size and location of the primary dorsal infraorbital foramen.

753

754

755

756

757

758

759

760

Figure 1(on next page)

Type locality of *Metopocetus hunteri*

Figure 1. Type locality of *Metopocetus hunteri*. Drawing of cetotheriid by Carl Buell.

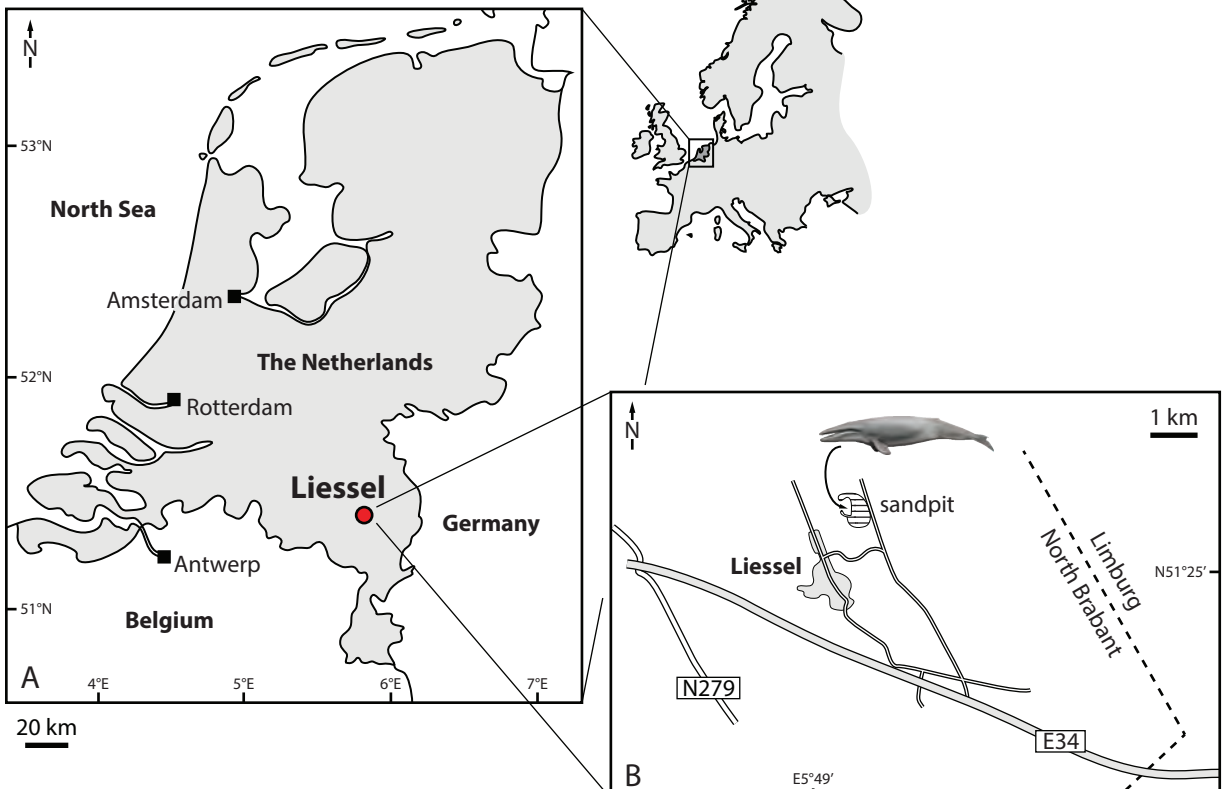
N
53°N
North Sea
Amsterdam
The Netherlands
52°N
Rotterdam
Liessel
Germany
Antwerp
51°N
Belgium
A
4°E
5°E
6°E
7°E
20 km
N
1 km
sandpit
Liessel
Limburg
North Brabant
N51°25′
N279
E34
B
E5°49′

Figure 2(on next page)

Cranium in dorsal view

Figure 2. Cranium of *Metopocetus hunteri* in (A) dorsal and (B) posterolateral view.

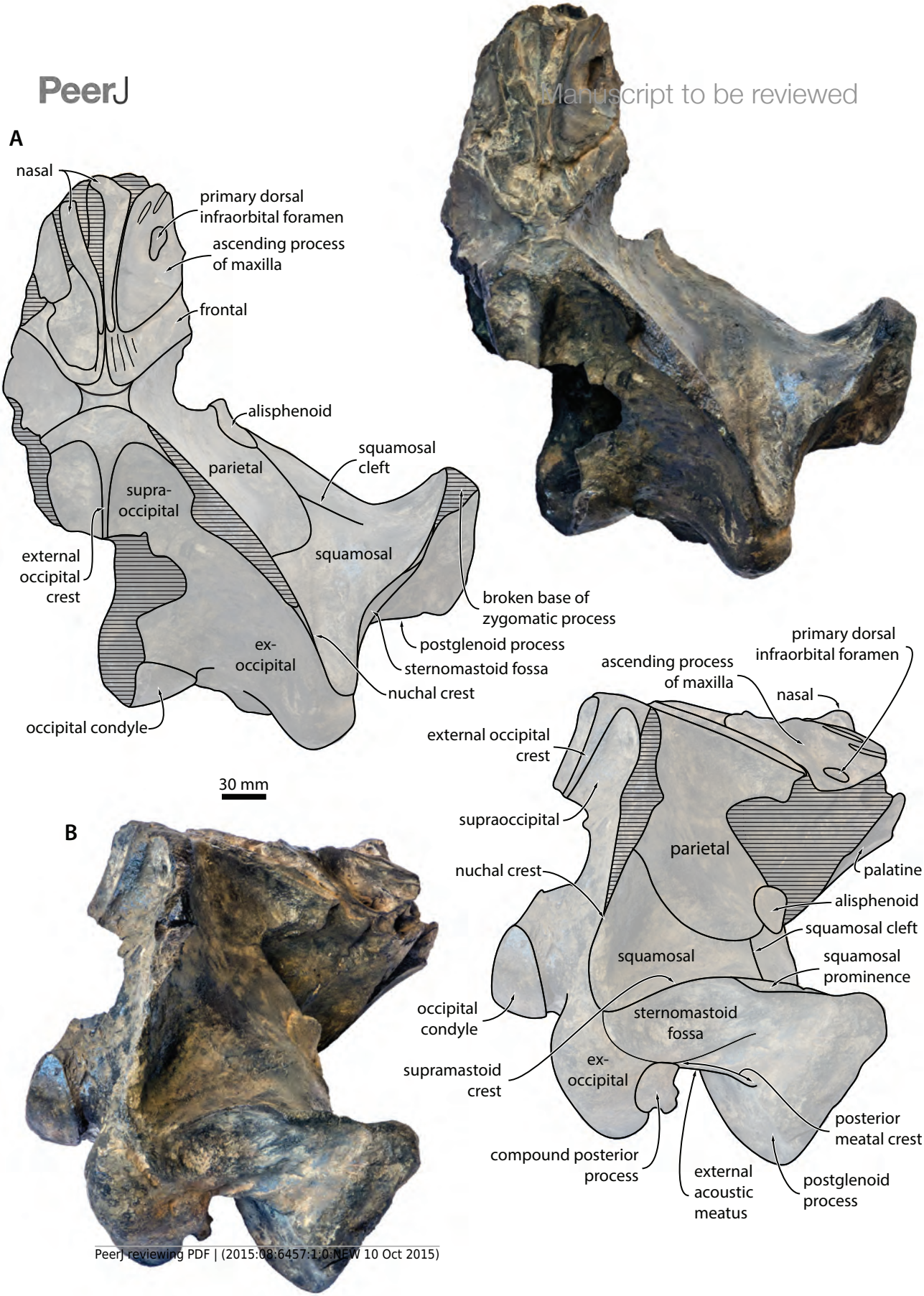
A
nasal
primary dorsal infraorbital foramen
ascending process of maxilla
frontal
alisphenoid
squamosal cleft
parietal
supra-occipital
squamosal
external occipital crest
broken base of zygomatic process
postglenoid process
sternomastoid fossa
ex-occipital
nuchal crest
occipital condyle
30 mm
B
primary dorsal infraorbital foramen
ascending process of maxilla
nasal
external occipital crest
supraoccipital
parietal
nuchal crest
palatine
alisphenoid
squamosal cleft
squamosal
squamosal prominence
occipital condyle
sternomastoid fossa
supramastoid crest
ex-occipital
posterior meatal crest
compound posterior process
external acoustic meatus
postglenoid process

Figure 3(on next page)

Temporal fossa and vertex

Figure 3. Detail of the cranium of *Metopocetus hunteri*: (A) posteromedial wall of temporal fossa in anteromedial view; (B) vertex in anterodorsal view.

A

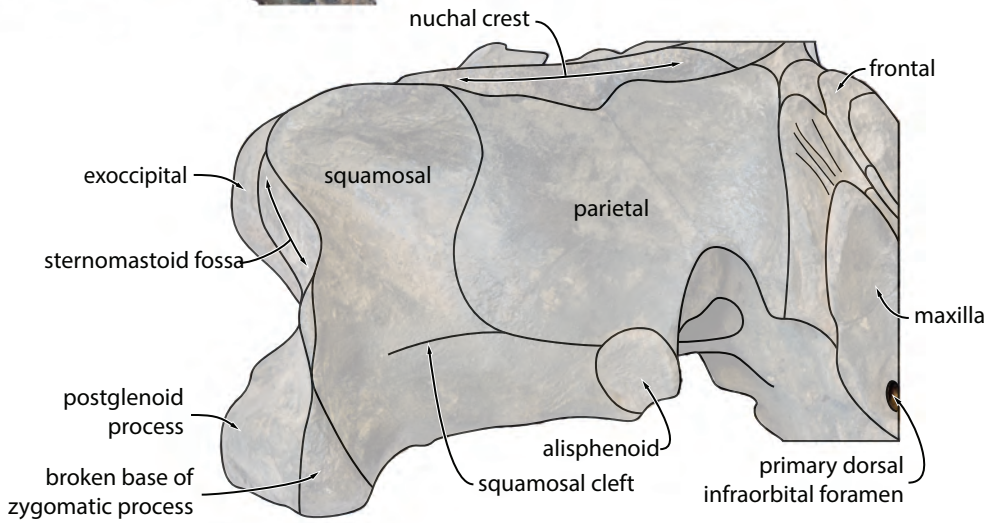

B

30 mm

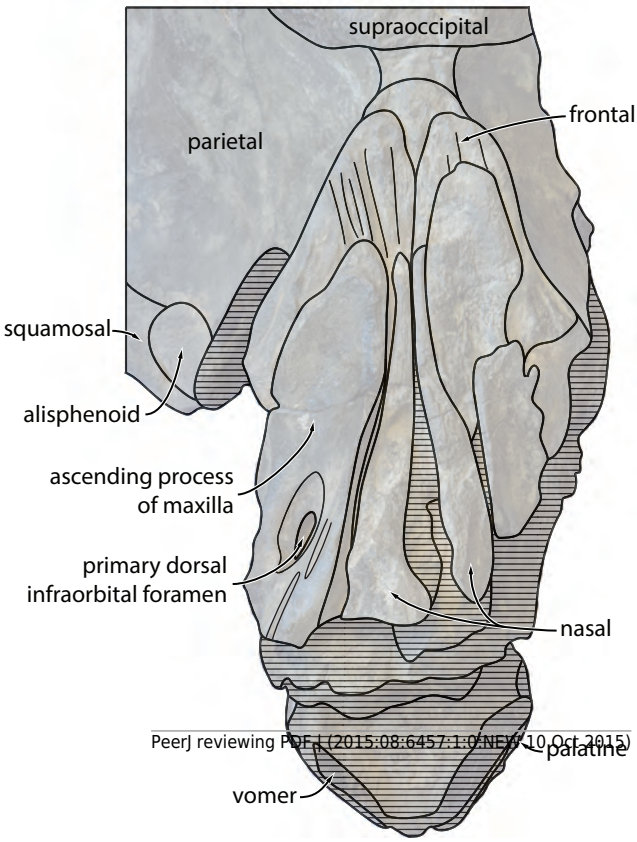

Figure 4(on next page)

Cranium in lateral and posterior view

Figure 4. Cranium of *Metopocetus hunteri* in (A) lateral and (B) posterior view.

A

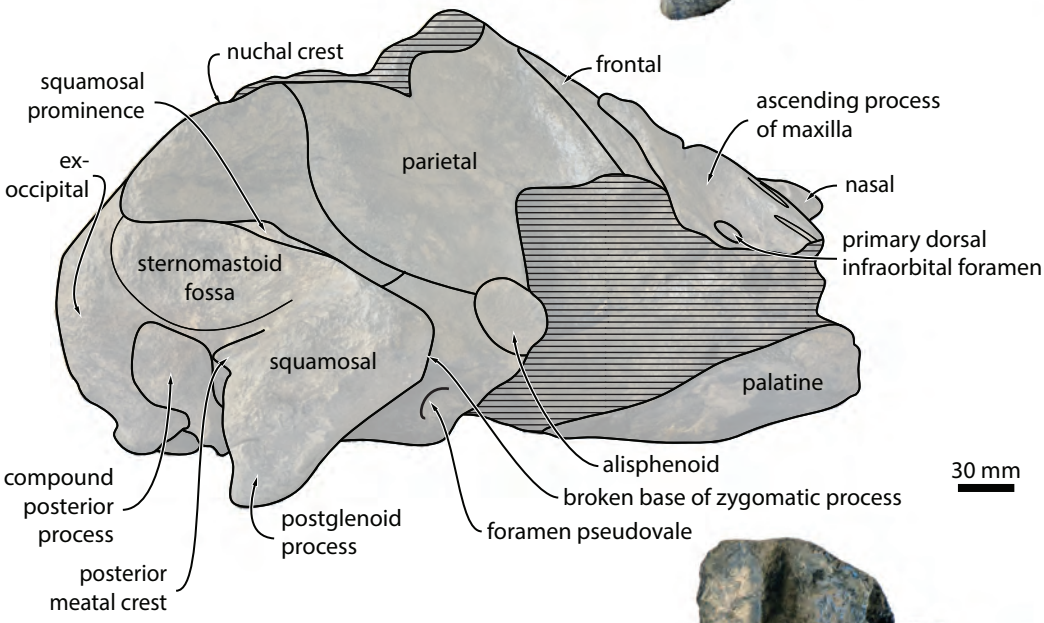

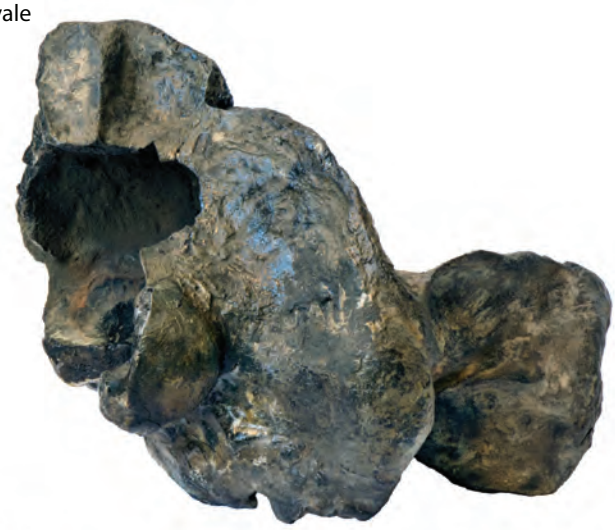

B

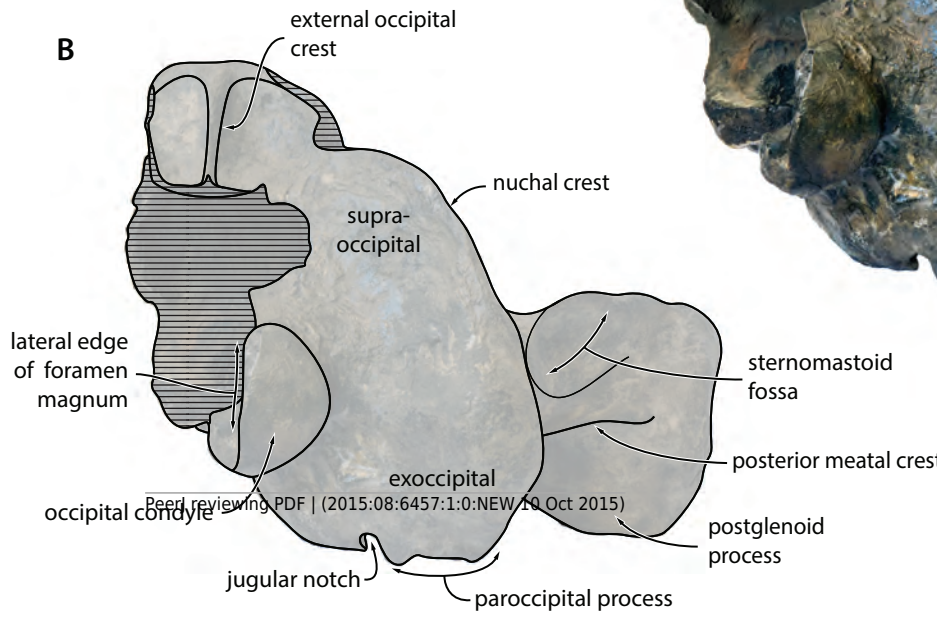

Figure 5(on next page)

Cranium in ventral view

Figure 5. Cranium of *Metopocetus hunteri* in ventral view.

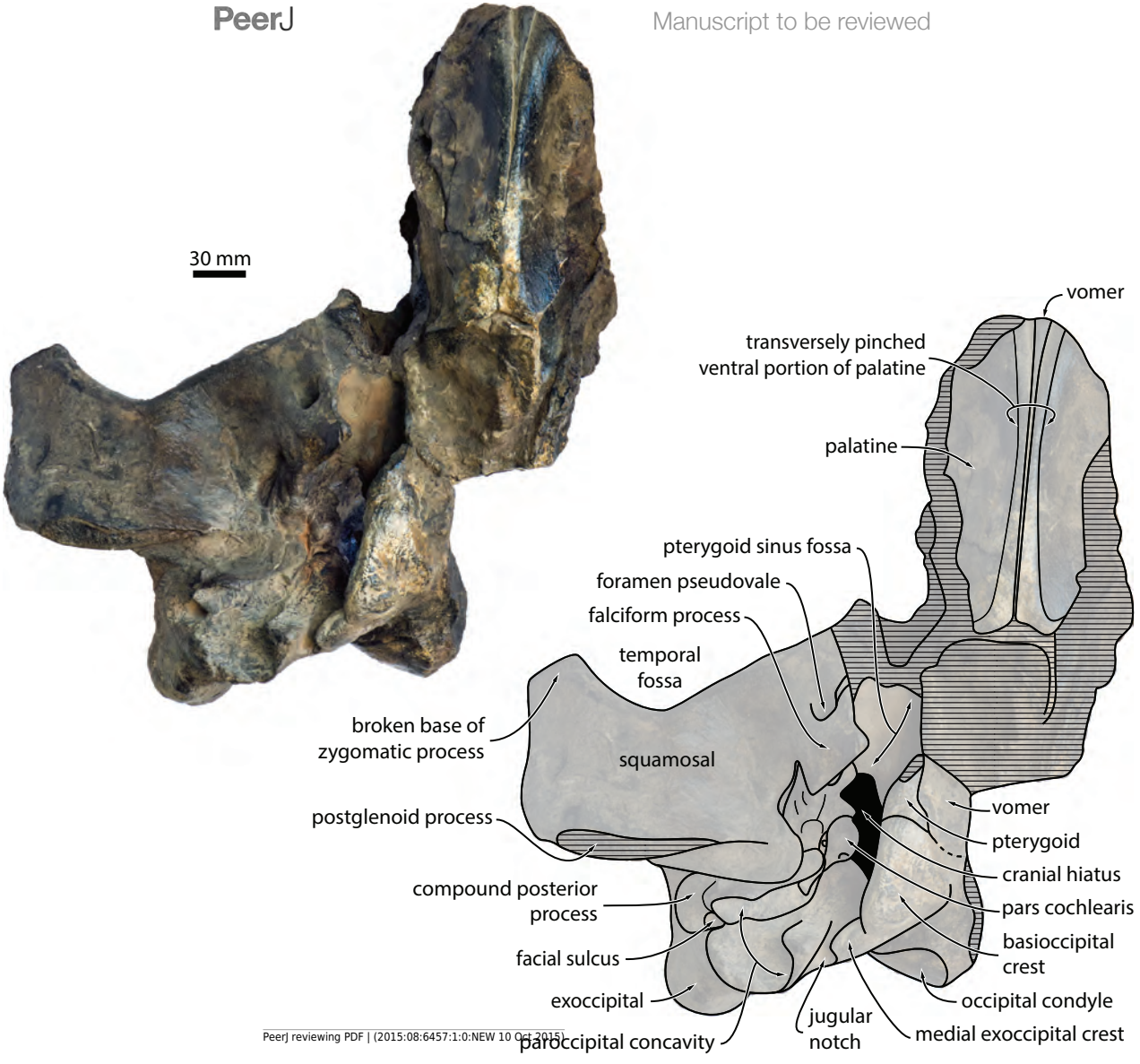
30 mm
vomer
transversely pinched ventral portion of palatine
palatine
pterygoid sinus fossa
foramen pseudovale
falciform process
temporal fossa
broken base of zygomatic process
squamosal
postglenoid process
vomer
pterygoid
cranial hiatus
pars cochlearis
compound posterior process
basioccipital crest
facial sulcus
exoccipital
occipital condyle
jugular notch
medial exoccipital crest
paroccipital concavity

Figure 6(on next page)

Basicranium and periotic

Figure 6. Basicranium and periotic of *Metopocetus hunteri*: (a) right portion of basicranium in ventral view; (b) central portion of periotic in ventromedial view; (c) compound posterior process of tympanoperiotic in external view; (d) central portion of periotic in dorsal view. Abbreviations: fac., facial sulcus; parocc. conc., paroccipital concavity; post. process, compound posterior process.

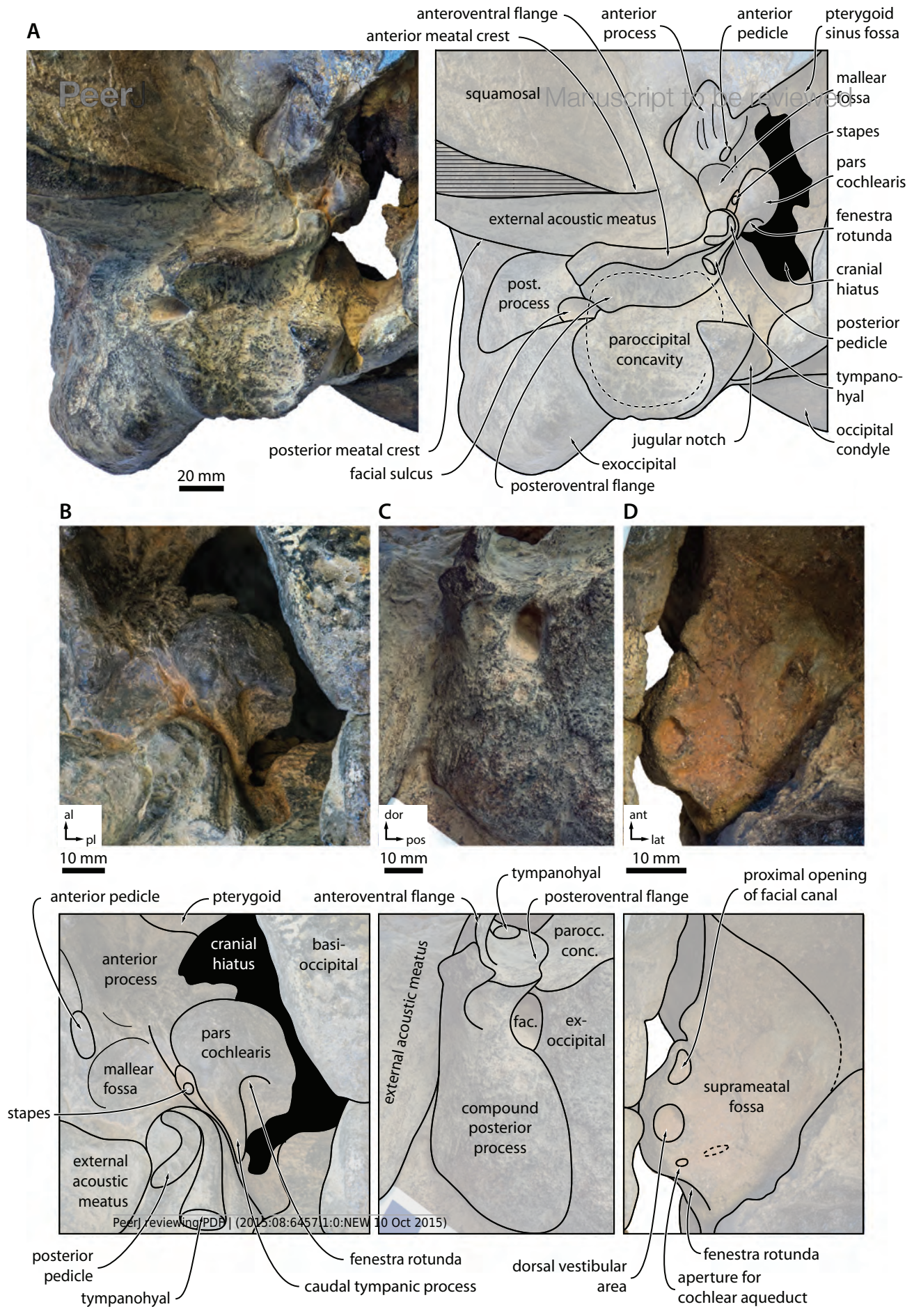

Figure 7 (on next page)

Tympanic bulla - photographs

Figure 8(on next page)

Tympanic bulla - explanatory line drawings

Figure 7 - continued

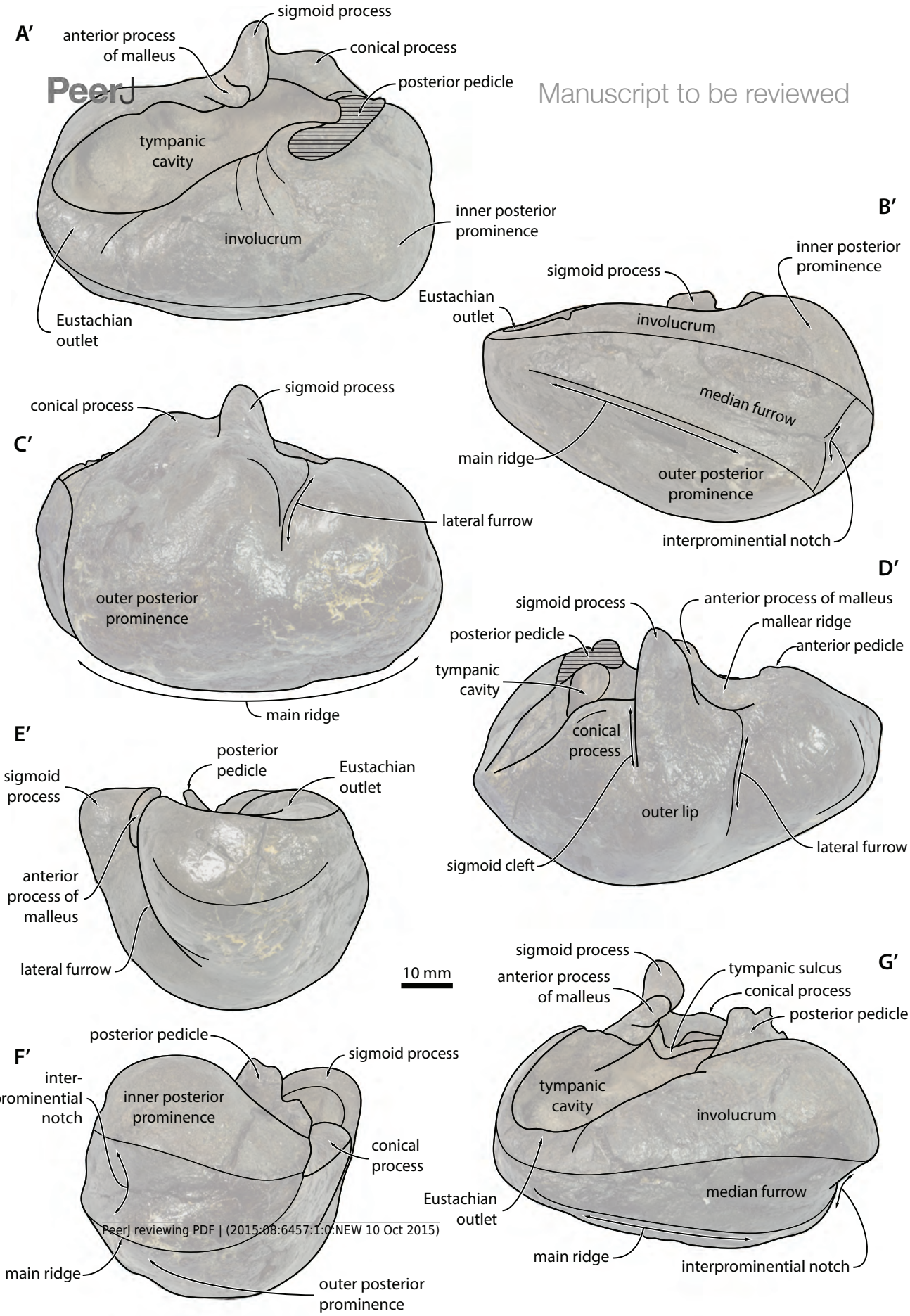

Figure 9(on next page)

Malleus

Figure 8. Malleus of *Metopocetus hunteri* in (A) posterior and (B) anterior view.

Abbreviations: dor, dorsal; med, medial; ven, ventral.

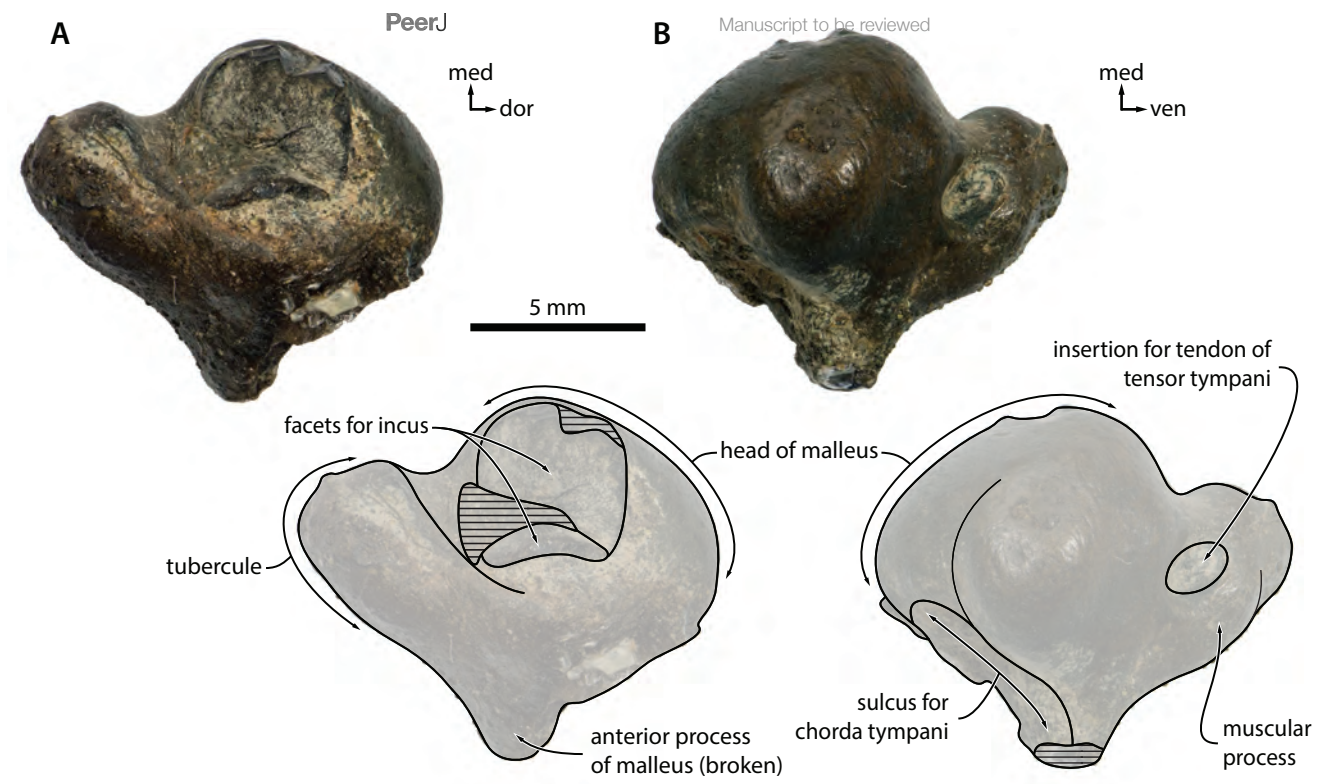
A
med
dor
B
med
ven
5 mm
facets for incus
head of malleus
tubercule
anterior process
of malleus (broken)
insertion for tendon of
tensor tympani
sulcus for
chorda tympani
muscular
process

Figure 10(on next page)

Phylogenetic relationships of Metopocetus hunteri

Figure 9. Phylogenetic relationships of *Metopocetus hunteri*, based on a dated total evidence analysis. All data except the codings for *M. hunteri* are from Marx & Fordyce (2015: fig. 2). Drawings of cetaceans by Carl Buell. Abbreviations: Pli., Pliocene; Pls., Pleistocene.

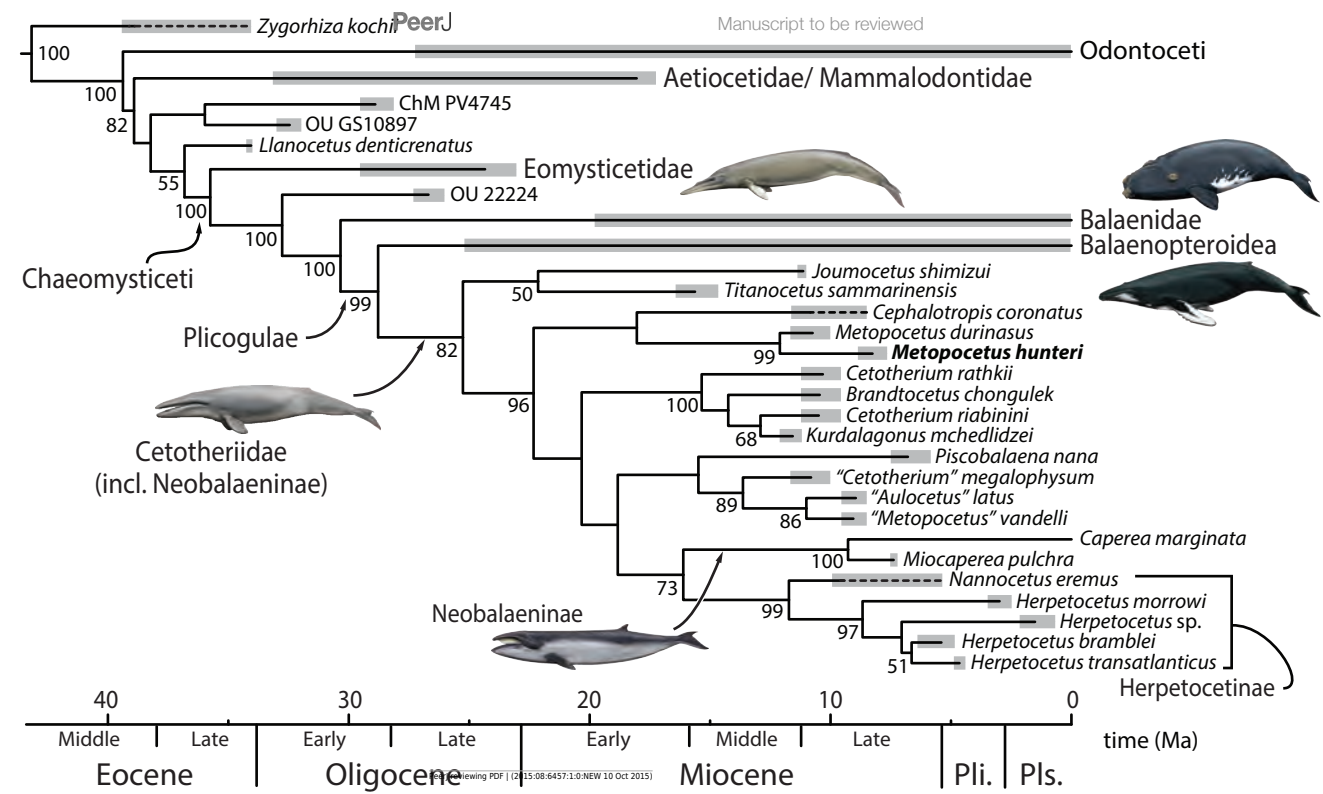
Zygorhiza kochii
Odontoceti
Aetiocetidae/ Mammalodontidae
ChM PV4745
OU GS10897
Llanocetus denticrenatus
Eomysticetidae
OU 22224
Balaenidae
Balaenopteroidea
Chaeomysticeti
Joumocetus shimizui
Titanocetus sammarinensis
Plicogulae
Cephalotropis coronatus
Metopocetus durinasus
Metopocetus hunteri
Cetotherium rathkii
Brandtocetus chongulek
Cetotherium riabinini
Kurdalagonus mchedlidzei
Cetotheriidae
(incl. Neobalaeninae)
Piscobalaena nana
"Cetotherium" megalophysum
"Aulocetus" latus
"Metopocetus" vandelli
Caperea marginata
Miocaperea pulchra
Nannocetus eremus
Herpetocetus morrowi
Herpetocetus sp.
Neobalaeninae
Herpetocetus bramblei
Herpetocetus transatlanticus
Herpetocetinae
40
30
20
10
0
Middle
Late
Early
Late
Early
Middle
Late
time (Ma)
Eocene
Oligocene
Miocene
Pli.
Pls.

Figure 11 (on next page)

Differences between *Metopocetus hunteri* and "*M.*" *vandelli*

Figure 10. Morphological features distinguishing "*Metopocetus*" *vandelli* from *M. durinasus* and *M. hunteri*. Crania in dorsal view.

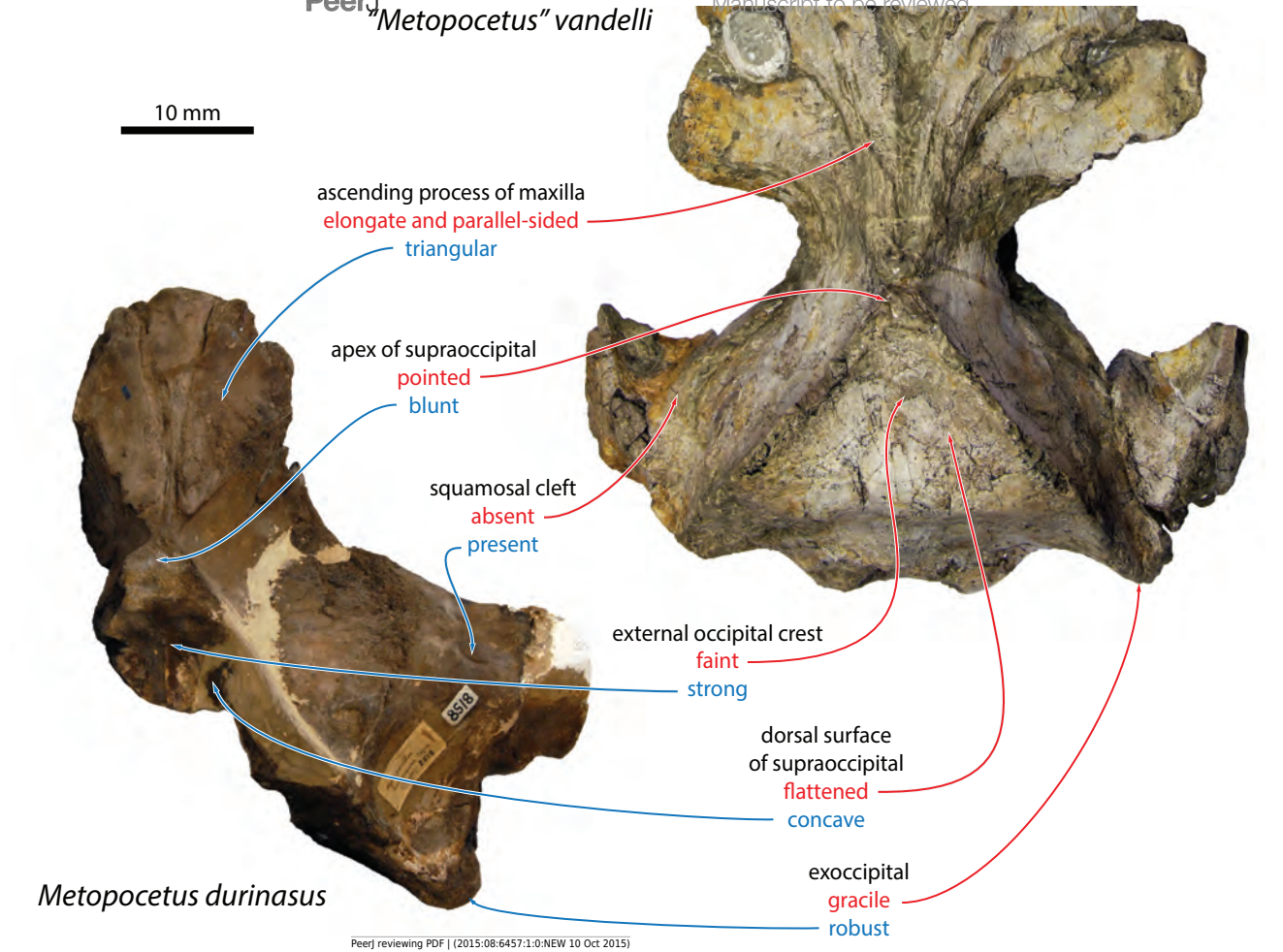
"Metopocetus" vandelli
10 mm
ascending process of maxilla
elongate and parallel-sided
triangular
apex of supraoccipital
pointed
blunt
squamosal cleft
absent
present
external occipital crest
faint
strong
dorsal surface
of supraoccipital
flattened
concave
exoccipital
gracile
robust
8518
Metopocetus durinasus

Figure 12(on next page)

Basicranium of *Eschrichtius robustus*

Figure 11. Left portion of the basicranium of the extant grey whale *Eschrichtius robustus* (USNM 364973) in ventrolateral view, highlighting the position of the paroccipital concavity.

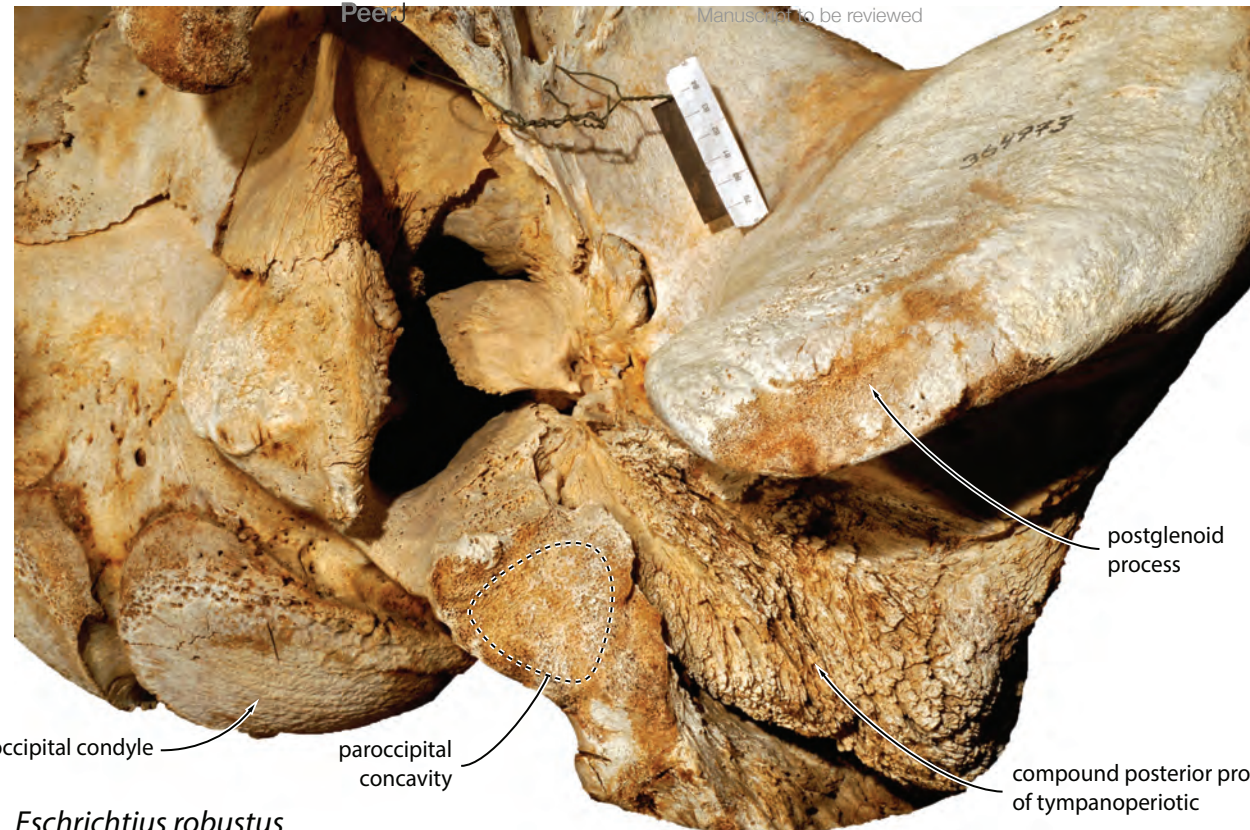

Eschrichtius robustus

Figure 13 (on next page)

Primary dorsal infraorbital foramen of various cetotheriids

Figure 12. Vertex of the cetotheriids *Piscobalaena nana* (MNHN SAS1616), *Herpetocetus morrowi* (UCMP 124950) and *"Metopocetus" vandelli* (MUHNAC A1) in dorsal view, showing the size and location of the primary dorsal infraorbital foramen.


Piscobalaena nana
Herpetocetus morrowi
"Metopocetus" vandelli
30 mm
20 mm
20 mm
primary dorsal
infraorbital foramen

Table 1(on next page)

Measurements of *Metopocetus hunteri*

Table 1 Measurements of *Metopocetus hunteri* (in mm).

1 **Table 1** Measurements of *Metopocetus hunteri* (in mm)

Cranium excluding ear bones	
Maximum length of right nasal, as preserved	137.0+
Maximum length of left nasal, as preserved	155.0
Anteroposterior diameter of primary dorsal infraorbital foramen	27.0
Transverse diameter of primary dorsal infraorbital foramen	14.5
Length of sulcus continuing posteriorly from primary dorsal infraorbital foramen	13.0
Length of slit-like sulcus on ascending process of maxilla, anteromedial to primary dorsal infraorbital foramen	25.0
Minimum transverse width across parietals on vertex	30.5
Maximum distance between sagittal plane and outer surface of the zygomatic process, as preserved	285.0
Maximum distance between sagittal plane and lateral border of the exoccipital	190.0
Anteroposterior length of pterygoid sinus fossa	64.0
Transverse width of pterygoid sinus fossa	56.0
Transverse width of postglenoid process at base	124
Maximum diameter of foramen pseudovale	20.0
Distance from posteromedial corner of falciform process of squamosal to innermost portion of internal acoustic meatus	32.5
Anteroposterior diameter of external acoustic	28.0

meatus	
Transverse width of basioccipital crest	47.0
Transverse width of jugular notch	10.7
Maximum anteroposterior diameter of paroccipital concavity	60.0
Maximum transverse diameter of paroccipital concavity	56.0
Maximum height of foramen magnum	51.0*
Maximum height of right occipital condyle	87.0
Maximum width of right occipital condyle	47.2
Bicondylar width*	150.0
Periotic and tympanohyal	
Anteroposterior length of anterior pedicle	9.0
Maximum anteroposterior width of pars cochlearis, measured up to the medial border of the fenestra rotunda	18.6
Maximum diameter of fenestra rotunda	5.8
Maximum diameter of proximal opening of facial canal	7.0
Maximum diameter of dorsal vestibular area	7.0
Maximum diameter of aperture for cochlear aqueduct	4.0
Maximum anteroposterior diameter of facial sulcus	9.7
Maximum dorsoventral diameter of facial sulcus	11.5
Anteroposterior length of lateral exposure of compound posterior process	33.0
Maximum proximodistal length of tympanohyal	22.3

Maximum diameter of distal surface of tympanohyal	7.3
Tympanic bulla and malleus	
Maximum anteroposterior length of tympanic bulla	77.1
Anteroposterior length of dorsal aperture of tympanic cavity	56.0
Width of bulla just anterior to the sigmoid process	47.3
Transverse width of sigmoid process	17.3
Transverse width of conical process	8.1
Maximum length of posterior pedicle	16.7
Maximum height of malleus, from the head to the tip of the tubercule	11.7
Maximum dorsoventral length of head of malleus	7.6

2 * estimated

3